



OPEN ACCESS

EDITED BY

Goichi Miyoshi,
Gunma University, Japan

REVIEWED BY

Katsuhiko Tabuchi,
Shinshu University, Japan
Dongqing Shi,
University of Michigan, United States

*CORRESPONDENCE

Jasmina N. Jovanovic
✉ j.jovanovic@ucl.ac.uk

RECEIVED 25 April 2024

ACCEPTED 02 July 2024

PUBLISHED 18 July 2024

CITATION

Sui Y, Mortensen M, Yuan B, Nicholson MW, Smart TG and Jovanovic JN (2024) GABA_A receptors and neuroligin 2 synergize to promote synaptic adhesion and inhibitory synaptogenesis.
Front. Cell. Neurosci. 18:1423471.
doi: 10.3389/fncel.2024.1423471

COPYRIGHT

© 2024 Sui, Mortensen, Yuan, Nicholson, Smart and Jovanovic. This is an open-access article distributed under the terms of the [Creative Commons Attribution License \(CC BY\)](https://creativecommons.org/licenses/by/4.0/). The use, distribution or reproduction in other forums is permitted, provided the original author(s) and the copyright owner(s) are credited and that the original publication in this journal is cited, in accordance with accepted academic practice. No use, distribution or reproduction is permitted which does not comply with these terms.

GABA_A receptors and neuroligin 2 synergize to promote synaptic adhesion and inhibitory synaptogenesis

Yusheng Sui¹, Martin Mortensen², Banghao Yuan¹,
Martin W. Nicholson¹, Trevor G. Smart² and
Jasmina N. Jovanovic^{1*}

¹Department of Pharmacology, School of Pharmacy, University College London, London, United Kingdom, ²Department of Neuroscience, Physiology and Pharmacology, Division of Biosciences, University College London, London, United Kingdom

GABA_A receptors (γ -aminobutyric acid-gated receptors type A; GABA_ARs), the major structural and functional postsynaptic components of inhibitory synapses in the mammalian brain, belong to a family of GABA-gated Cl⁻/HCO₃⁻ ion channels. They are assembled as heteropentamers from a family of subunits including: α (1–6), β (1–3), γ (1–3), δ , ϵ , π , θ and ρ (1–3). GABA_ARs together with the postsynaptic adhesion protein Neuroligin 2 (NL2) and many other pre- and post-synaptic proteins guide the initiation and functional maturation of inhibitory GABAergic synapses. This study examined how GABA_ARs and NL2 interact with each other to initiate the formation of synapses. Two functionally distinct GABA_AR subtypes, the synaptic type $\alpha 2\beta 2\gamma 2$ -GABA_ARs versus extrasynaptic type $\alpha 4\beta 3\delta$ -GABA_ARs were expressed in HEK293 cells alone or together with NL2 and co-cultured with striatal GABAergic medium spiny neurons to enable innervation of HEK293 cells by GABAergic axons. When expressed alone, only the synaptic $\alpha 2\beta 2\gamma 2$ -GABA_ARs induced innervation of HEK293 cells. However, when GABA_ARs were co-expressed with NL2, the effect on synapse formation exceeded the individual effects of these proteins indicating a synergistic interaction, with $\alpha 2\beta 2\gamma 2$ -GABA_AR/NL2 showing a significantly greater synaptogenic activity than $\alpha 4\beta 3\delta$ -GABA_AR/NL2 or NL2 alone. To investigate the molecular basis of this interaction, different combinations of GABA_AR subunits and NL2 were co-expressed, and the degree of innervation and synaptic activity assessed, revealing a key role of the $\gamma 2$ subunit. In biochemical assays, the interaction between NL2 and $\alpha 2\beta 2\gamma 2$ -GABA_AR was established and mapped to the large intracellular domain of the $\gamma 2$ subunit.

KEYWORDS

inhibition, GABAergic synapse, synaptic, extrasynaptic, stable cell lines, medium spiny neurons, immunocytochemistry, protein domains

1 Introduction

GABA_A receptors are the essential structural and functional postsynaptic components of inhibitory synapses in the mammalian brain. They belong to a diverse family of GABA-gated Cl⁻/HCO₃⁻ permeable ion channels that promote neuronal differentiation and synaptogenesis in the developing brain by increasing neuronal excitability (Owens and Kriegstein, 2002;

Raimondo et al., 2017; Cherubini and Ben-Ari, 2023). In contrast, in the adult brain, GABA_ARs mediate inhibitory neurotransmission by decreasing neuronal excitability in a process that is fundamental to normal brain function and information processing (Schofield et al., 1987; Olsen and Sieghart, 2009; Smart and Stephenson, 2019; Sallard et al., 2021).

GABA_ARs are hetero-pentameric assemblies of subunits selected from: α (1–6), β (1–3), γ (1–3), δ , ϵ , π , θ and ρ (1–3), in which two α , two β and one γ subunit are required for the formation of fully functional synaptic receptors (Olsen and Sieghart, 2009; Chua and Chebib, 2017; Scott and Aricescu, 2019). The subtypes of GABA_ARs which incorporate α 1-3 and 5, β 2-3 and γ 2 subunits are spatially, functionally, and pharmacologically distinct from those containing the α 4, 6, β 2-3 and δ subunits (Farrant and Nusser, 2005; Smart and Mortensen, 2023). The presence of the γ 2 subunit is obligatory for synaptic GABA_ARs because it governs their localization and clustering at the postsynaptic membrane, allowing for the rapid and robust neurotransmission in all GABAergic synapses (Olsen and Sieghart, 2009; Lorenz-Guertin et al., 2018). However, the γ 2-containing GABA_ARs translocate in and out of synapses as part of their lifecycle. Thus, they are not solely a synaptic feature, but do also transit through the extrasynaptic space (Thomas et al., 2005; Hannan et al., 2020). In contrast, the subtypes of GABA_ARs lacking the γ 2 subunit ($\alpha\beta$ isoforms), or those incorporating the δ subunit are predominantly located outside of synapses where they can be activated by low levels of ambient GABA to mediate tonic inhibition (Farrant and Nusser, 2005; Smart and Mortensen, 2023). While the incorporation of the β subunit is required for the expression of GABA_ARs at the neuronal cell surface (Connolly et al., 1996a,b; Nguyen and Nicoll, 2018), some α subunits are selectively assembled at specific inhibitory synapses where they support the formation and function of neuronal circuits involved in specific brain physiology, such as anxiety, sedation, arousal, and others (Klausberger et al., 2002; Rudolph and Mohler, 2006; Thomson and Jovanovic, 2010).

How, where, and when inhibitory synapses are formed is tightly regulated during brain development by genetic and environmental factors and guided by specialized protein–protein interactions leading to the formation of transsynaptic complexes between the pre- and postsynaptic elements. Multiple proteins have been shown to participate in the initiation and functional maturation of inhibitory synapses, including the postsynaptic adhesion protein NL2 together with its presynaptic partners α and β neurexins (Sudhof, 2017; Sudhof, 2018; Ali et al., 2020), as well as other synaptic partners, such as SLITRK3, β -dystroglycan, IgSF9b, GARLH4/LHFPL4 (Connor and Siddiqui, 2023). GABA_ARs themselves participate in inhibitory synaptogenesis as structural (Fuchs et al., 2013; Brown et al., 2014, 2016; Duan et al., 2019) and signaling (Pallotto and Deprez, 2014; Arama et al., 2015; Cherubini and Ben-Ari, 2023) components and contribute to the functional specialization of synapses via the incorporation of specific receptor subtypes with distinct physiological properties (Thomson and Jovanovic, 2010; Fritschy et al., 2012; Fritschy and Panzanelli, 2014).

Constitutive and inducible gene knockout studies of individual proteins involved in synapse formation in mice, including NL2, have revealed subtle deficits in inhibitory synapses, without causing a global impairment of GABAergic synaptogenesis (Fritschy et al., 2012; Sudhof, 2018). This suggests that the process of synapse initiation and functional maturation relies on multiple protein

complexes and, importantly, their specific interactions which incrementally and cooperatively contribute to this process. While molecular details of these interactions remain largely unknown, their importance has been demonstrated in the developing hippocampus where cooperative interaction between NL2 and SLITRK3 is required for the formation and functional maturation of inhibitory synapses (Li et al., 2017).

Our initial studies have demonstrated a cooperative interaction between GABA_ARs and NL2 in promoting the formation and strengthening of synaptic connections in a co-culture model in which HEK293 cells expressing GABA_ARs and NL2 were cultured together with GABAergic medium spiny neurons (Fuchs et al., 2013). Here, we have explored this cooperativity further to uncover the molecular details of the GABA_AR/NL2 interaction. Our experiments demonstrate that the prototypical synaptic α 2 β 2 γ 2-GABA_ARs have a significantly greater effect in facilitating the NL2-dependent induction of synapses than the prototypical extrasynaptic α 4 β 3 δ -GABA_ARs. Furthermore, we demonstrate that the synergism between GABA_ARs and NL2 is mediated by the γ 2 subunit interaction with NL2, and we map this interaction to the intracellular domain of this subunit.

2 Materials and methods

2.1 Cell lines, primary neuronal cultures and co-cultures

Human embryonic kidney cells (ATCC) were maintained using Dulbecco's Minimum Essential Medium (DMEM; Thermo Fischer) supplemented with 10% v/v fetal bovine serum (FBS; 10082–147, Thermo Fischer), 10 mM L-Glutamine (25030–024, Thermo Fischer), 50 units/mL penicillin and 50 μ g/mL streptomycin (15140–148, Thermo Fischer). HEK293 cell lines stably expressing GABA_ARs were kept in complete DMEM with the addition of 800 μ g/mL Geneticin G418 sulfate (11811023, Thermo Fischer), 800 μ g/mL Zeocin (R25001, Gibco), and 800 μ g/mL hygromycin B (10687010, Invitrogen) for selection of α 2 and α 4 subunits, β 2 and β 3 subunits, and γ 2 and δ subunits, respectively. The α 2 β 2 γ 2-GABA_AR stable cell line was described previously (Brown et al., 2014) and in Supplementary Figure S1.

The GABAergic medium spiny neuron cultures were prepared from the striatum of ~ day E17 embryonic Sprague–Dawley rats (UCL-BSU) housed and sacrificed according to United Kingdom Home Office guidelines as previously described (Brown et al., 2014). Briefly, brains were dissected in sterile Ca²⁺ and Mg²⁺-free HEPES-buffered saline solution (HBSS; 14180–046, Thermo Fischer) to obtain striata. Neurons were dissociated using fire-polished Pasteur glass pipettes, counted using a hemocytometer, and plated onto poly-D-lysine (0.1 mg/mL, P1149-10MG, Sigma Aldrich) coated tissue culture dishes (Z707686, TPP) for biochemical experiments, or poly-L-lysine (0.1 mg/mL, P6282-5MG, Sigma Aldrich) coated 13 mm glass coverslips (631-0148P, VWR) for immunolabeling and electrophysiology. Neuronal cultures and co-cultures with HEK293 cells were maintained in Neurobasal medium (21103–049, Gibco) containing B27 supplement (17504–044, Gibco), glutamine (2 mM, 25030–024, Gibco), penicillin (50 units/mL, 15070–63, Gibco), streptomycin (50 g/mL, 15070–063, Gibco), and glucose (6 mM, G8769, Sigma).

In order to generate a HEK293 neuronal co-culture, adherent HEK293 cells (control or stably expressing GABA_ARs) were first transfected with the cDNA of proteins of interest using Effectene (301425, Qiagen), and 24 h later these cells were transferred to the medium spiny neuron culture for a further 24–48 h of incubation, as described previously (Brown et al., 2014).

2.2 Construction of HEK293 cell line stably expressing $\alpha 4\beta 3\delta$ -GABA_ARs

GABA_AR $\alpha 4$, $\beta 3$ and δ cDNAs were cloned into pcDNA3-G418 (Invitrogen), pcDNA3.1-zeocin (Invitrogen) and pcDNA3.1-hygromycin (Invitrogen), respectively, for antibiotic-selective expression. Lipofectamine LTX (15338–030, Invitrogen) was used for the two-stage stable transfection. For the first stage, $\alpha 4$ and $\beta 3$ cDNAs were transfected into HEK293 cells followed by G418 and zeocin antibiotic selection. For the second stage, the HEK293 cell line clone expressing both subunits was transfected with δ cDNA followed by G418, zeocin, and hygromycin antibiotic selection. Stable expression of the subunits was confirmed by immunoblotting and immunolabeling using subunit-specific antibodies and their functional properties were assessed using whole-cell recordings (Supplementary Figure S2).

2.3 Cell surface ELISA

HEK293 cells stably expressing GABA_ARs were transfected with HA-tagged NL2 cDNA (Poulopoulos et al., 2009) using Effectene (301,425, Qiagen), and incubated in 24-well plates coated with 0.1 mg/mL poly-D-lysine (P1149, Sigma Aldrich) in the 37°C 5% CO₂ humidified incubator for 24 h. The cells were fixed with 4% paraformaldehyde (PFA)/4% sucrose w/v in PBS for 10 min at room temperature and subsequently washed with PBS and HBSS (14185–052, Gibco). Cells were blocked in 1% bovine serum albumin (BSA, BP9704-100, Fisher Scientific) in HBSS for 30 min at room temperature and subsequently incubated with anti-HA tag primary antibody (1,10,000 in blocking solution, ab184643, Abcam) for 2 h at room temperature or overnight at 4°C. For assessing the total expression of proteins, cells were permeabilized with 0.5% Triton X-100 (A16046, Alfa-Aesar) in HBSS for 10 min at room temperature before the blocking step. After incubation, cells were washed, blocked in 1% BSA in HBSS for 30 min at room temperature, and incubated with the secondary antibody conjugated to horseradish peroxidase (HRP) (31,460, Thermo Fisher) in 1% BSA/ HBSS (1,2,500) for 1 h at room temperature. The cells were washed with HBSS and the HRP activity was detected using tetramethylbenzidine reagent (TMB, 34028, Thermo Scientific). The oxidation of TMB produced blue color, the absorbance of which was measured at 650 nm by DU800 spectrophotometer (Beckman Coulter).

2.4 Immunocytochemistry

The cells plated on 13 mm coverslips coated with poly-L-lysine were briefly washed with PBS and fixed with 4% PFA/4% sucrose in PBS for 10 min at room temperature. For assessing the activity of the

presynaptic terminals, Cy5-labeled anti-synaptotagmin 1 luminal domain-specific antibody (1,50, 105311C5, Synaptic Systems) was added to the culture and incubated in the 37°C 5% CO₂ humidified incubator for 30 min before fixation. The PFA was aspirated, and the cells were washed thoroughly with PBS. The residual aldehyde groups of PFA were blocked with 0.3 M glycine in PBS for 10 min at room temperature, followed by multiple washes with PBS. The cells were blocked in 1% BSA in PBS for 30 min at room temperature. The primary antibodies: anti-VGAT (1,500, 131,003, Synaptic Systems), anti-GABA_AR $\alpha 2$ subunit (1,500, 224,103, Synaptic Systems), anti-GABA_AR $\alpha 4$ subunit (1,200, Hörtnagl et al., 2013), anti-GABA_AR $\beta 2/3$ subunit (1,500, MAB341, Sigma Aldrich), anti-GABA_AR $\gamma 2$ subunit (1,2,500, Fritschy and Mohler, 1995), anti-GABA_AR δ subunit (1,200, 868-GDN, PhosphoSolutions), and anti-Bassoon (1,500, MA1-20689, Thermo Fischer) were diluted in 1% BSA in PBS, added to the cells, and incubated for 2 h at room temperature or overnight at 4°C. After incubation, the cells were rinsed twice and washed multiple times with PBS. For labeling of intracellular proteins, the cells were permeabilized with 0.5% Triton-X-100 in PBS for 10 min at room temperature prior to the addition of the primary antibody mix. The cells were washed and blocked again with 1% BSA in PBS for 30 min at room temperature. Fluorescently-labeled secondary antibodies (AlexaFluor, Invitrogen) were diluted in 1% BSA in PBS (1,750) and added to the cells for 1 h at room temperature protected from light. The coverslips were washed with PBS and mounted on glass slides with ProLong Gold antifade reagent (P36930, Invitrogen). The slides were dried at room temperature protected from light and kept at 4°C in boxes.

2.5 Confocal imaging and analysis

The coverslips were imaged using a Zeiss confocal microscope LSM 700, 710, or 880 with 63× oil immersion objective and analyzed using ImageJ (National Institute of Health) as described previously (Brown et al., 2016). Images were acquired at 12-bit depth from 10 to 15 cells from each co-culture. For each image, a series of z-stack images were acquired from the bottom to the top of HEK293 cells with optimal intervals of 0.7 μ m. ImageJ software was utilized for the analysis of contacts formed between presynaptic GABAergic terminals of cultured neurons and HEK293 cells. The co-localization was obtained by the *Process* → *Image Calculator* function using the option *and* which produced an image showing all the pixels that appeared in both channels. The threshold of the image was adjusted by the *Auto-Threshold* function. The data for co-localization were obtained by the *Analyze* → *Analyze Particles* function. For quantitative assessment of synaptic contacts formed between presynaptic GABAergic terminals and HEK293 cells, the % *area* was selected because this parameter represents the surface area of each HEK293 cell with co-localized pixels normalized to the total surface area of the cell, which therefore accounts for the difference in size of individual HEK293 cells. These parameters were imported into Origin Pro software for statistical analysis and graphical presentation of the data. The data were plotted with Box-and-Whisker plots showing the median, standard deviation, and outliers. The normal (Gaussian) distribution of the data was first tested using the Shapiro–Wilk normality test. Non-normally distributed data were subjected to non-parametric Mann–Whitney test or Kruskal Wallis ANOVA followed by Dunn's test for multiple

comparisons. Normally distributed data were analyzed using a two-tailed Student's t-test to determine the statistical significance.

2.6 Super-resolution imaging and analysis

The samples were prepared in the same way as for the confocal imaging. The GABA_ARs were labeled with $\alpha 2$ (1,500, 224,103, Synaptic Systems) or $\alpha 4$ (1,200, Hörtnagl et al., 2013) subunit-specific antibodies, respectively. The synaptic contacts were labeled with presynaptic active zone marker Bassoon-specific antibody (MA1-20689, Thermo Fischer). Images were acquired using ELYRA PS.1 SIM (Carl Zeiss) at 63x oil lens following chromatic shift correction by recording fluorescent beads. A 4 μm z-stack with 0.110 μm intervals of the samples was acquired to keep the z-range in focus. The images were then processed by the Structured Illumination and Channel Alignment function in Zen 2012 Software. The images were deconvolved and analyzed using SVI Huygens Professional software. After deconvolution, the background was eliminated using the Costes Optimized method (Coastes et al., 2004). The z-stack images were rendered to 3-dimensional images for colocalization analysis and Manders coefficients were calculated to show the level of overlapping signals, with M1 indicating the proportion of Bassoon overlapping with GABA_ARs and M2 indicating the proportion of GABA_ARs overlapping with Bassoon.

2.7 Immunoblotting

Cultured cells were lysed with 2% SDS and the protein concentration determined using the BCA assay (Thermo Fisher Scientific). Proteins were separated on 10% SDS-poly-acrylamide separation gels and transferred onto a solid nitrocellulose membrane (Whatman). For the detection of proteins, the following primary antibodies were used: anti-HA tag (1,1,000, ab184643, Abcam), anti-GABA_AR $\alpha 1$ subunit (1,500, Duggan and Stephenson, 1990), anti-GABA_AR $\beta 3$ subunit (1:200, UCL 74, (Tretter et al., 1997)), anti-GABA_AR δ subunit (1,200, 868-GDN, PhosphoSolutions) and anti NL2 (1,800, 129,203, Synaptic Systems). Anti-alkaline phosphatase-conjugated secondary antibodies: anti-rabbit (1,1,000, A16099, Invitrogen) and anti-mouse (1,200, 31,450, Invitrogen) were used for visualization of the protein bands.

2.8 Co-immunoprecipitation

Protein lysates were obtained from adult male rat cortex or HEK293 cells expressing GABA_ARs/NL2 via homogenization in lysis buffer (20 mM HEPES pH 7.4, 100 mM NaCl, 1% Triton X-100, 2 mM CaCl₂, 1 mM MgCl₂), containing phenylmethylsulfonyl fluoride (PMSF; 10 μM), leupeptin, chymostatin, pepstatin (5 $\mu\text{g}/\text{mL}$ each, Peptide Institute). The concentration of the protein lysates was determined by Bradford assay (Bio-Rad). The input (1 mg total protein) was incubated with 10 μg of GABA_AR $\alpha 1$ or $\alpha 2$ subunit-specific antibodies (Duggan and Stephenson, 1990), or anti-HA tag (ab184643, Abcam) or anti-c-myc antibody (2 $\mu\text{g}/\text{mL}$, 05-724, Millipore) or non-immune control antibodies (31,243, Invitrogen, from the same species as the specific antibody) followed by 1% BSA

coated Protein-G-Sepharose beads (50 μL , NB-45-00037-5, Generon). The beads were pulled down by centrifugation after extensive washing and denatured with Laemmli SB (62.5 mM Tris, pH 8.0, 2% SDS, 10% glycerol, 0.0025% Bromophenol Blue, 100 mM DTT) for SDS/PAGE and immunoblotting.

2.9 Electrophysiology

Coverslips with cells (transfected HEK293, stable HEK293 cell lines, neurons or HEK293/neuron co-cultures) were transferred into a recording chamber on a Nikon Eclipse FN1 microscope, where cells were continuously perfused with Krebs solution containing (mM): 140 NaCl, 4.7 KCl, 1.2 MgCl₂, 2.52 CaCl₂, 11 Glucose and 5 HEPES (pH 7.4). Patch pipettes (thin-walled filamented borosilicate glass capillaries; TW150F-4; WPI, United States; 3–4 M Ω) were filled with an intracellular solution containing (mM): 140 CsCl, 2 NaCl, 2 MgCl₂, 5 EGTA, 10 HEPES, 0.5 CaCl₂, 2 Na-ATP and 0.5 Na-GTP (pH 7.2). To record functional current GABA_AR responses, drugs were applied to cells using a Y-tube delivery system (Mortensen and Smart, 2007).

HEK293 cells were voltage-clamped at -40 mV using an Axopatch 200B amplifier (Molecular Devices, United States), and whole-cell currents (IPSCs or drug-activated) were filtered at 5 kHz (-36 dB), digitized at 50 kHz via a Digidata 1322A (Molecular Devices), and recorded to a Dell Optiplex 990 using Clampex 10.2 (Molecular Devices). Series resistance was compensated at 70%, and only data with less than 20% deviation in series resistance was included in subsequent analyses.

3 Results

3.1 Synergistic interaction between GABA_ARs and NL2 in synapse formation

We have demonstrated previously that stable expression of synaptic $\alpha 1\beta 2\gamma 2$ -GABA_ARs in HEK293 cells promotes the adhesion of GABAergic axons and the formation of functional synapses when these cells are co-cultured with the GABAergic medium spiny neurons (Fuchs et al., 2013; Brown et al., 2014, 2016). When GABA_ARs were co-expressed with NL2 in this system, the effect on synapse formation exceeded the individual effects of these two proteins both in the number and transmission efficacy of the synapses ascertained by electrophysiological recordings (Fuchs et al., 2013). To investigate the degree of HEK293 cell innervation induced by another synaptic GABA_AR type and possible synergistic interaction with NL2, in the current study, we have expressed and functionally characterized the HEK293 stable cell line expressing the $\alpha 2\beta 2\gamma 2$ -GABA_AR (Supplementary Figures S1A,B; Brown et al., 2014). These cells were fluorescently labeled by transiently expressing the green fluorescent protein (GFP) and co-cultured with GABAergic medium spiny neurons (Figure 1A). The control HEK293 cells were also labeled with GFP. The cells were fixed and immunolabeled with a VGAT-specific antibody to detect GABAergic terminals forming contacts with HEK293 cells using confocal microscopy. Synaptic contacts were defined based on signal colocalization between the VGAT and GFP (green and blue channels in Figure 1A) and analyzed using Image J as described in the Methods and previously (Brown et al., 2014).

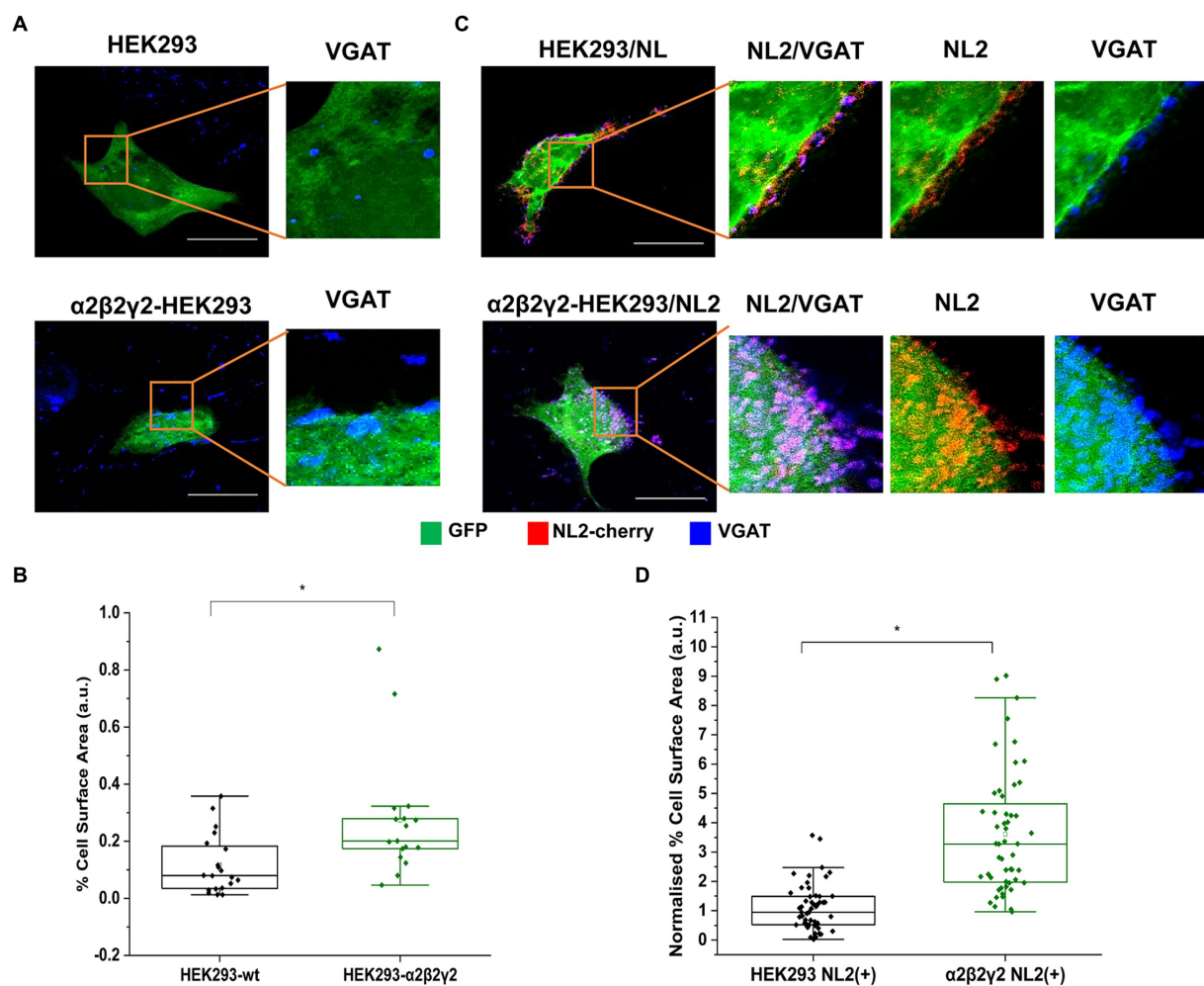


FIGURE 1

$\alpha 2\beta 2\gamma 2$ -GABA_ARs induce synaptic contact formation and potentiate the induction of contacts by NL-2. Synaptic contact formation in co-culture of embryonic medium spiny neurons and (A) HEK293 (wt; upper panels) or $\alpha 2\beta 2\gamma 2$ -GABA_AR-expressing HEK293 cells (lower panels), or (C) HEK293/NL2 cells (wt; upper panels) or $\alpha 2\beta 2\gamma 2$ -GABA_AR/NL2-expressing cells (lower panels). The HEK293 cell body was visualized by GFP (green), GABAergic terminals were labeled with an anti-VGAT antibody (blue) and NL2 was mcherry-tagged (red). Scale bar = 20 μ m. Fluorescent imaging was done using Zeiss 700 confocal microscope at 63 \times magnification with image size 1,024 \times 1,024. Max intensity projection of the z-stack images was shown. The enlarged images are 10 \times zoom in. Quantitative analysis of synapses expressed as % area of co-localized pixels that represent contacts between VGAT terminals and in (B) HEK293 or $\alpha 2\beta 2\gamma 2$ -GABA_AR-expressing cells ($n = 21$ and $n = 18$, respectively; $N = 2$ independent experiments, $p = 0.002$), or (D) HEK293/NL2 cells or $\alpha 2\beta 2\gamma 2$ -GABA_AR/NL2 expressing cells ($n = 53$ and $n = 52$ cells, respectively; $N = 3$ independent experiments, $p < 0.00001$ (4.7×10^{-13})). The box and whisker plot show the mean (square dot with no fill), median (horizontal line), and standard deviation (whiskers). Shapiro–Wilk normality test was used to test the normal distribution of the data and Mann–Whitney test was used to analyze statistical significance of the difference ($*p < 0.05$).

Quantification of the % area of co-localized pixels that represent contacts between VGAT terminals and HEK293 cells revealed a significant increase in synaptic contact formation in the presence of $\alpha 2\beta 2\gamma 2$ -GABA_ARs in comparison with the control HEK293 cell line (median = 0.20%; IQR = 0.16 - 0.30%; $n = 17$ cells vs. median = 0.08%; IQR = 0.03 - 0.21%; $n = 21$ cells, respectively; from $N = 2$ independent experiments, $p = 0.002$, Figure 1B).

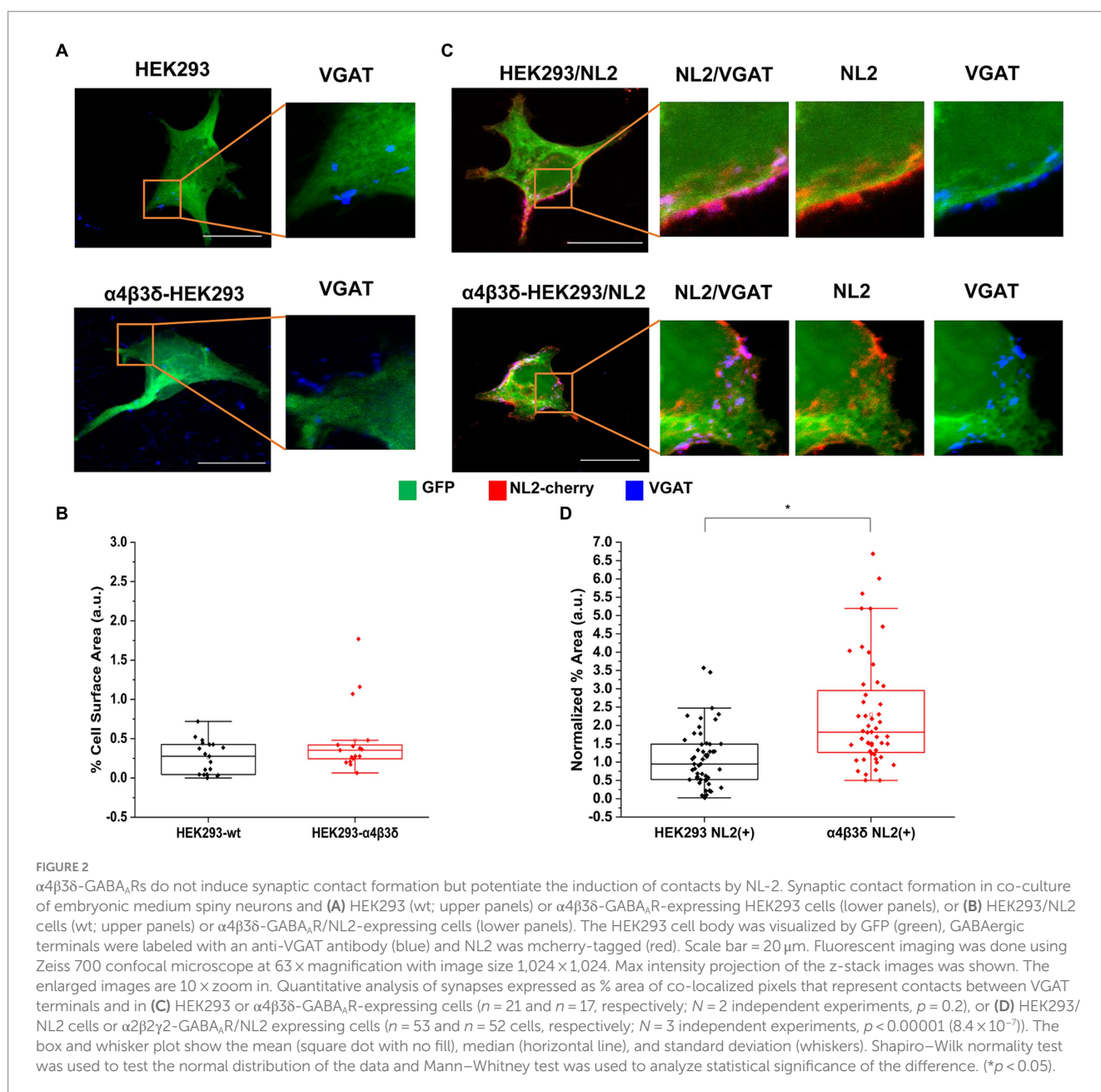
To investigate how the co-expression of GABA_ARs and NL2 in HEK293 cells may regulate the formation of synaptic contacts, HEK293 cells stably expressing $\alpha 2\beta 2\gamma 2$ -GABA_ARs or the control HEK293 cells were transfected with GFP and cherry-tagged NL2 cDNAs, and co-cultured with the medium spiny neurons (Figure 1C). Expression of NL2 in control HEK293 cells induced synaptic contact formation in agreement with the published literature [median = 0.95%;

IQR = 0.52 - 1.49%; $n = 53$ cells from $N = 3$ independent experiments; $p < 0.00001$ ($p = 3.5 \times 10^{-9}$); (Scheiffele et al., 2000) but when NL2 was expressed in the $\alpha 2\beta 2\gamma 2$ -GABA_AR stable cell line, the formation of contacts was significantly greater [median = 3.28%; IQR = 1.96 - 4.78%; $n = 52$ cells from $N = 3$ independent experiments; $p < 0.00001$ ($p = 4.7 \times 10^{-13}$); Figure 1D]. In this analysis, the value of the % area of co-localized pixels for each HEK293 cell was divided by the fluorescence value of NL2 measured in the same cell because of the high degree of variation in expression of NL2 following transient transfection. These results support the previously described (Fuchs et al., 2013) strong synergistic interaction between GABA_ARs and NL2 during the formation of synaptic contacts.

The $\alpha 4\beta 3\delta$ -GABA_ARs are generally localized outside of GABAergic synapses and they mediate tonic inhibition (Farrant and

Nusser, 2005). These receptors were also expressed in HEK293 cells to create a stable cell line which was characterized using immunolabeling and voltage-clamp electrophysiology. The ubiquitous expression of all three subunits at the cell surface was confirmed by confocal imaging (Supplementary Figures S2A,B). Pharmacological responses of these receptors to GABA and the modulator DS2 ($\alpha\beta\delta$ specific) in whole-cell recordings indicated that the receptors expressing the δ subunit were functional (Supplementary Figures S2C,D). To test whether these receptors can induce the adhesion of GABAergic terminals, the HEK293 cell line or control HEK293 cells were transiently transfected with GFP and co-cultured with the medium spiny neurons (Figure 2A). Quantification of the % area of co-localized pixels which represents contacts between VGAT terminals and HEK293 cells demonstrated no significant difference between the control and $\alpha\beta\delta$ -GABA_AR HEK293 cells (median = 0.28%; IQR = 0.04–0.42%;

$n = 19$ cells vs. median = 0.35%; IQR = 0.23–0.45%; $n = 17$ cells, respectively; from $N = 2$ independent experiments, $p = 0.2$, Figure 2B). These results indicate that $\alpha\beta\delta$ -GABA_ARs do not promote the formation of inhibitory synapses in these cultures, indicating that this activity is a characteristic of the synaptic GABA_AR subtypes (Brown et al., 2016). However, when $\alpha\beta\delta$ -GABA_AR-HEK293 cells or control HEK293 cells were transiently transfected with GFP and cherry-tagged NL2 cDNAs and co-cultured with the medium spiny neurons (Figure 2C), we detected a significant increase in contacts induced by NL2 in the presence of $\alpha\beta\delta$ -GABA_ARs (median = 1.81%; IQR = 1.25 - 3.02%; $n = 52$ cells versus the no $\alpha\beta\delta$ expressing control median = 0.95%; IQR = 0.52 - 1.49%; $n = 53$ cells, respectively; from $N = 3$ independent experiments; $p < 0.00001$ ($p = 8.4 \times 10^{-7}$); Figure 2D). The value of the % area of co-localized pixels for each cell was normalized to the expression of NL2 as described above. These



results indicate that extrasynaptic GABA_ARs can facilitate the NL2-dependent induction of synapses although their effect is significantly weaker than the effect observed for synaptic GABA_ARs.

To test whether the observed potentiation of NL2 effects by GABA_ARs may be a consequence of increased expression of NL2, we have transfected the HA-tagged NL2 cDNA into the control, $\alpha 4\beta 3\delta$ -GABA_AR- or $\alpha 2\beta 2\gamma 2$ -GABA_AR-expressing HEK293 cells and carried out ELISA using an HA tag-specific antibody (Supplementary Figure S3). However, the surface or total expression of NL2 showed no difference between these conditions, indicating that other molecular mechanisms may mediate the observed cooperative interaction between NL2 and GABA_ARs.

The GABA_AR- and NL2- induced synaptic contacts were further characterized using immunolabeling and super-resolution imaging to measure the degree of co-localization between the $\alpha 2\beta 2\gamma 2$ -GABA_ARs or $\alpha 4\beta 3\delta$ -GABA_ARs and the presynaptic active vesicular release zone protein Bassoon. In these experiments, the $\alpha 2\beta 2\gamma 2$ -GABA_AR/NL2- or $\alpha 4\beta 3\delta$ -GABA_AR/NL2-expressing HEK293 cells in co-culture with the medium spiny neurons were immunolabeled with an $\alpha 2$ - or $\alpha 4$ -subunit-specific antibody, respectively, in combination with a Bassoon-specific antibody. While both GABA_AR subtypes showed predominantly punctate distribution at the cell surface, their colocalization with Basson-positive terminals appeared greater for the $\alpha 2\beta 2\gamma 2$ -GABA_AR than $\alpha 4\beta 3\delta$ -GABA_AR, which was in agreement with our confocal imaging data (Figures 3A,B). This was confirmed by a

significantly higher M1 coefficient value obtained for the Bassoon/ $\alpha 2\beta 2\gamma 2$ -GABA_AR co-localization in synaptic contacts than Bassoon/ $\alpha 4\beta 3\delta$ -GABA_ARs co-localization (median = 0.27; IQR = 0.24–0.42; $n = 8$ cells versus median = 0.17; IQR = 0.10–0.25; $n = 8$ cells, respectively; from $N = 2$ independent experiments, $p = 0.04$; Figure 3C). In contrast, the M2 coefficient appeared higher but without reaching significance for the $\alpha 2\beta 2\gamma 2$ -GABA_AR overlapping with Bassoon than the $\alpha 4\beta 3\delta$ -GABA_AR (median = 0.73; IQR = 0.24–0.81; $n = 8$ cells vs. median = 0.51; IQR = 0.36–0.66; $n = 8$ cells, respectively; from $N = 2$ independent experiments; Figure 3D). These results indicate that NL2-induced formation of synapses is more likely to occur in the proximity of the $\alpha 2\beta 2\gamma 2$ -GABA_AR than $\alpha 4\beta 3\delta$ -GABA_AR.

3.2 Structural and functional characterization of synaptic contacts induced by co-expression of GABA_ARs and NL2

Functional characterization of synaptic contacts formed with the control/NL2, $\alpha 2\beta 2\gamma 2$ -GABA_AR/NL2- or $\alpha 4\beta 3\delta$ -GABA_AR/NL2-expressing HEK293 cells was first carried out by assessing the activity of their presynaptic components, GABAergic terminals, in synaptotagmin-antibody uptake assay (Fernández-Alfonso, Kwan and

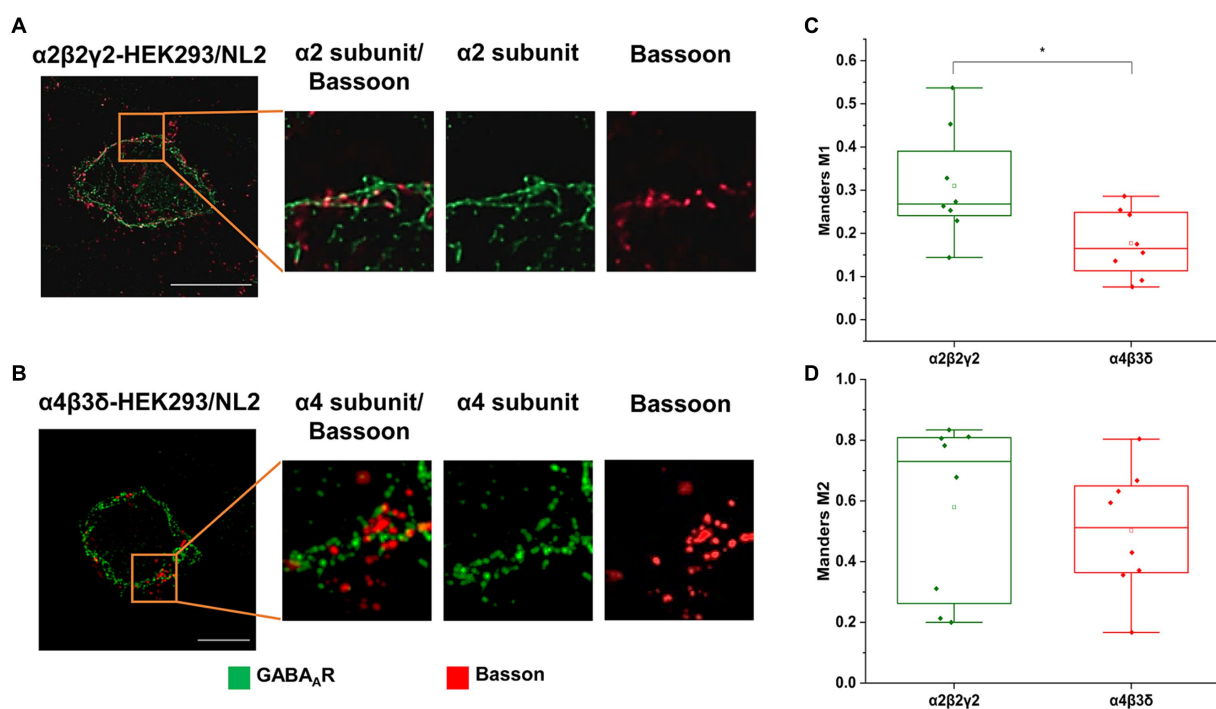


FIGURE 3

Co-localization of the presynaptic marker Bassoon and GABA_A receptors on the surface of (A) $\alpha 2\beta 2\gamma 2$ -GABA_AR, or (B) $\alpha 4\beta 3\delta$ -GABA_AR-expressing HEK293 cells in co-culture with the embryonic medium spiny neurons. GABA_AR $\alpha 2$ or $\alpha 4$ subunits (green) and Basson (red) were visualized using specific antibodies. Images were acquired using Zeiss ELYRA PS.1 SIM at 63 \times magnification. Scale bar = 10 μ m. (C,D) Quantitative analysis of colocalization between presynaptic marker Bassoon and GABA_AR $\alpha 2/4$ subunits using Manders' coefficient M1, which indicates the proportion of Bassoon signals that overlap with GABA_A receptor $\alpha 2/4$ subunits (C), and Manders' coefficient M2, which indicates the proportion of $\alpha 2/4$ subunit signals that overlap with Bassoon signals (D). The M1 coefficient is significantly higher in $\alpha 2\beta 2\gamma 2$ -GABA_AR/NL2 expressing cell than in $\alpha 4\beta 3\delta$ -GABA_AR/NL2 expressing cells (t-test, $p = 0.04$). The M2 coefficient is higher in $\alpha 2\beta 2\gamma 2$ -GABA_AR cells than in $\alpha 4\beta 3\delta$ -GABA_AR cells, but this difference is not statistically significant. Data from $n = 8$ cells from $N = 2$ independent experiments.

Ryan, 2006). In this assay, active presynaptic terminals were fluorescently labeled with a Cy5-tagged anti-synaptotagmin 1 vesicle-luminal domain-specific antibody (1,50, see Methods). The cells were fixed, permeabilized and immunolabeled with the VGAT-specific antibody, allowing us to visualize both active and inactive terminals forming contacts with HEK293 cells and quantify their ratio (Figures 4A–C). Quantification of the % area of co-localized pixels that represent contacts between synaptotagmin-positive and VGAT-positive terminals and the control HEK293 cells, confirmed that NL2 can induce the adhesion of active terminals in the absence of GABA_ARs (median = 0.12%; IQR = 0.03 - 0.22%; $n = 30$ cells; from $N = 3$ independent experiments; Figures 4A,D). However, in the presence of $\alpha 4\beta 3\delta$ -GABA_ARs, NL2 had a significantly greater effect (median = 0.52%; IQR = 0.18 - 0.95%; $n = 21$ cells; from $N = 2$ independent experiments, $p = 0.0006$; Figures 4B,D). Moreover, in the presence of $\alpha 2\beta 2\gamma 2$ -GABA_ARs, NL2 was even more effective and the number of active synapses was significantly larger [$p < 0.00001$ ($p = 6.4 \times 10^{-10}$)] than the number obtained in the absence of GABA_ARs or presence of $\alpha 4\beta 3\delta$ -GABA_ARs (median = 1.32%; IQR = 0.78 - 2.03%; $n = 21$ cells; from $N = 2$ independent experiments, $p = 0.04$, Figures 4C,D). The percentage of synapses incorporating active terminals in these experiments was ~10% (control/NL2), 24% ($\alpha 4\beta 3\delta$ -GABA_AR/NL2), and 30% ($\alpha 2\beta 2\gamma 2$ -GABA_AR/NL2).

Electrophysiological analysis of the whole-cell recordings of inhibitory postsynaptic currents (IPSCs) in GABA_AR- or GABA_AR/NL2 expressing HEK293 cells revealed that GABA-mediated synaptic transmission could be detected reproducibly only in the presence of the $\alpha 2\beta 2\gamma 2$ -GABA_ARs (Figure 5). In the absence of NL2, the IPSCs were detected in 60% of the $\alpha 2\beta 2\gamma 2$ -GABA_AR-HEK293 cells (Figures 5A,G,H; 9 out of 15), in which 8 cells were detected with <0.1 Hz IPSC and 1 cell with >0.1 Hz,

which supports the results of the structural analysis presented in Figure 1A. When NL2 was co-expressed, IPSCs were detected in 93.3% of $\alpha 2\beta 2\gamma 2$ -GABA_AR/HEK293 cells (14 out of 15), in which 2 cells were detected with <0.1 Hz IPSC and 12 cells with >0.1 Hz (Figures 5B,G,H). In the absence of NL2, no IPSCs were detected in the $\alpha 4\beta 3\delta$ -GABA_AR/HEK293 cells (11 cells, Figures 5D,G,H), while in the presence of NL2, IPSCs were detected in only 1 $\alpha 4\beta 3\delta$ -GABA_AR-HEK293 cell out of 15 (> 0.1 Hz; Figures 5E,G,H). These data show that expression of NL2 increases the frequency of GABAergic IPSCs in the presence of synaptic $\alpha 2\beta 2\gamma 2$ -GABA_ARs. However, synaptic contacts induced by NL2 alone or the presence of $\alpha 4\beta 3\delta$ -GABA_ARs (Figures 2–4) fail to differentiate into active synapses and remain functionally silent (~95% of cells; 1/15).

Given a clear difference in the number and activity of NL2-induced synaptic contacts in the presence of $\alpha 2\beta 2\gamma 2$ - and $\alpha 4\beta 3\delta$ -GABA_ARs, we were keen to establish which of the GABA_AR subunits may play a key role in these processes. To test different subunit combinations, we transiently transfected into the $\beta 3$ -expressing HEK293 stable cell line (B2 clone) combinations of $\alpha 2$, $\alpha 4$, $\gamma 2$ or δ subunits cDNAs to form the following GABA_AR subtypes: $\alpha 2\beta 3\gamma 2$, $\alpha 4\beta 3\delta$, $\alpha 4\beta 3\gamma 2$ or $\alpha 2\beta 3\delta$. These cells were also co-transfected with cherry-NL2 cDNA. The cells were co-cultured with medium spiny neurons and synaptic activity in HEK293 cells was examined using whole-cell recordings. Compared to the $\alpha 2\beta 2\gamma 2$ -GABA_AR/NL2-expressing HEK293 cells, a similar level of activity was detected in 7 out of 8 of the $\alpha 4\beta 3\gamma 2$ -GABA_AR/NL2-expressing HEK293 cells with IPSC frequencies >0.1 Hz (Figures 5C,G,H). However, in 8 out of 10 of the $\alpha 2\beta 3\delta$ -GABA_AR/NL2-expressing HEK293 cells, no IPSCs were detected, indicating that the majority of synaptic contacts formed in these conditions were also functionally silent (Figures 5F–H).

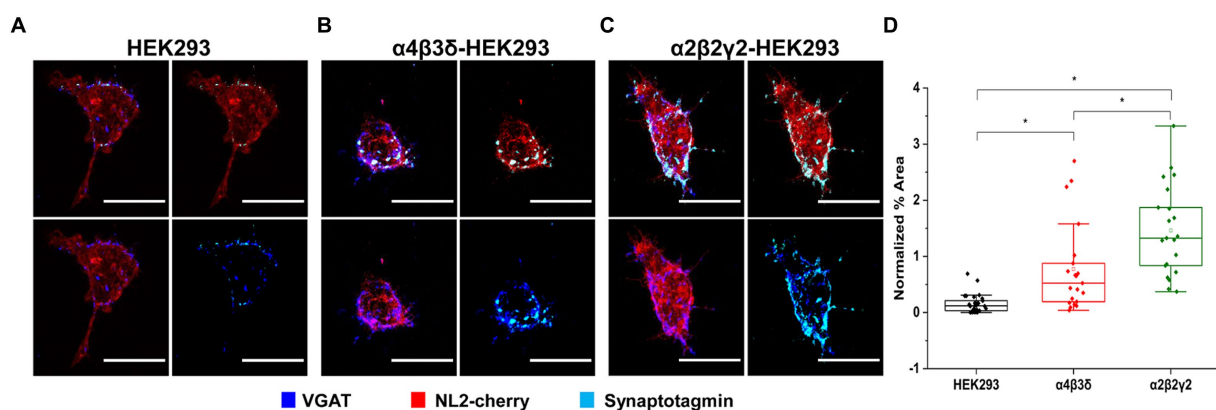
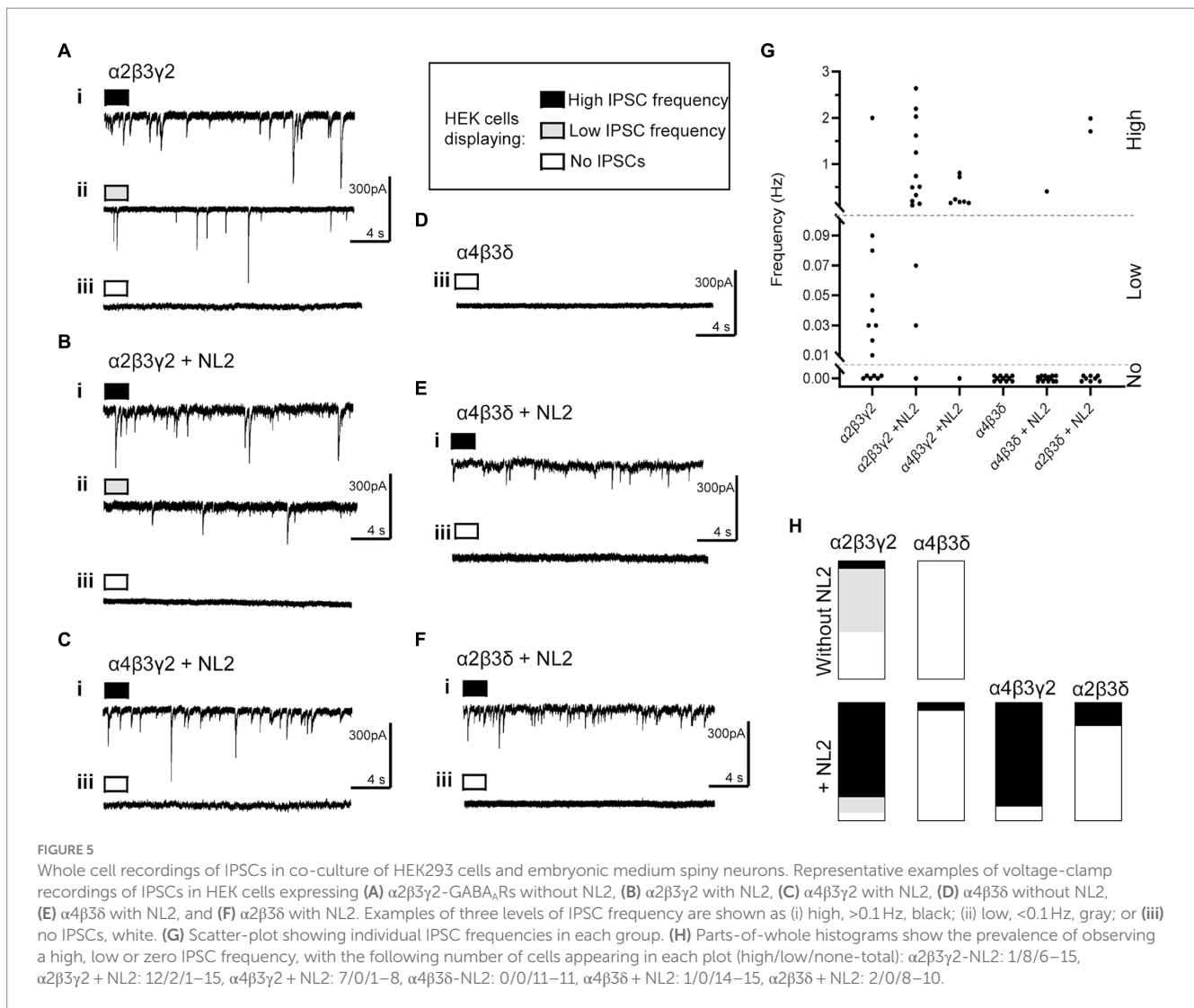


FIGURE 4

GABA_AR and NL2 co-expression induces the adhesion of active GABAergic terminals. Presynaptic activity is detected in synapses formed with (A) wt/NL2-expressing HEK293 cells, (B) $\alpha 4\beta 3\delta$ -GABA_AR/NL2-expressing HEK293 cells, or (C) $\alpha 2\beta 2\gamma 2$ /NL2-GABA_AR-expressing HEK293 cells in co-culture with embryonic medium spiny neurons. Active presynaptic terminals were visualized with the Cy5-labeled anti-synaptotagmin luminal domain-specific antibody (cyan), while all presynaptic terminals were visualized with an anti-VGAT-specific antibody (blue). NL2 was tagged with mCherry tag (red). Scale bar = 20 μ m. Fluorescent imaging was done using Zeiss 700 confocal microscope at 63x magnification with image size 512 x 512. Max intensity projection of the z-stack images was shown. The enlarged images are 10x zoom in. (D) Quantitative analysis of active synaptic contacts in which the % area was normalized to the expression level of NL2. The box and whisker plot shows the mean (square dot with no fill), median (horizontal line), and standard deviation of the mean (whiskers). Data from HEK293 cells ($n = 30$, from $N = 3$ independent experiments), $\alpha 4\beta 3\delta$ -GABA_AR-expressing HEK293 cells ($n = 22$, from $N = 2$ independent experiments) and $\alpha 2\beta 2\gamma 2$ -GABA_AR-expressing HEK293 cells ($n = 22$, from $N = 2$ independent experiments). Significant difference was detected between HEK293 cells and $\alpha 4\beta 3\delta$ -GABA_AR-expressing HEK293 cells ($p = 0.0006$), HEK293 cells and $\alpha 2\beta 2\gamma 2$ -GABA_AR-expressing HEK293 cells (6.4×10^{-10}) and $\alpha 4\beta 3\delta$ -GABA_AR-expressing HEK293 cells and $\alpha 2\beta 2\gamma 2$ -GABA_AR-expressing HEK293 cells ($p = 0.04$). Shapiro–Wilk normality test was used to test the normal distribution of the data and Kruskal Wallis ANOVA followed by Dunn's test was used to analyze the statistical significance ($*p < 0.05$).



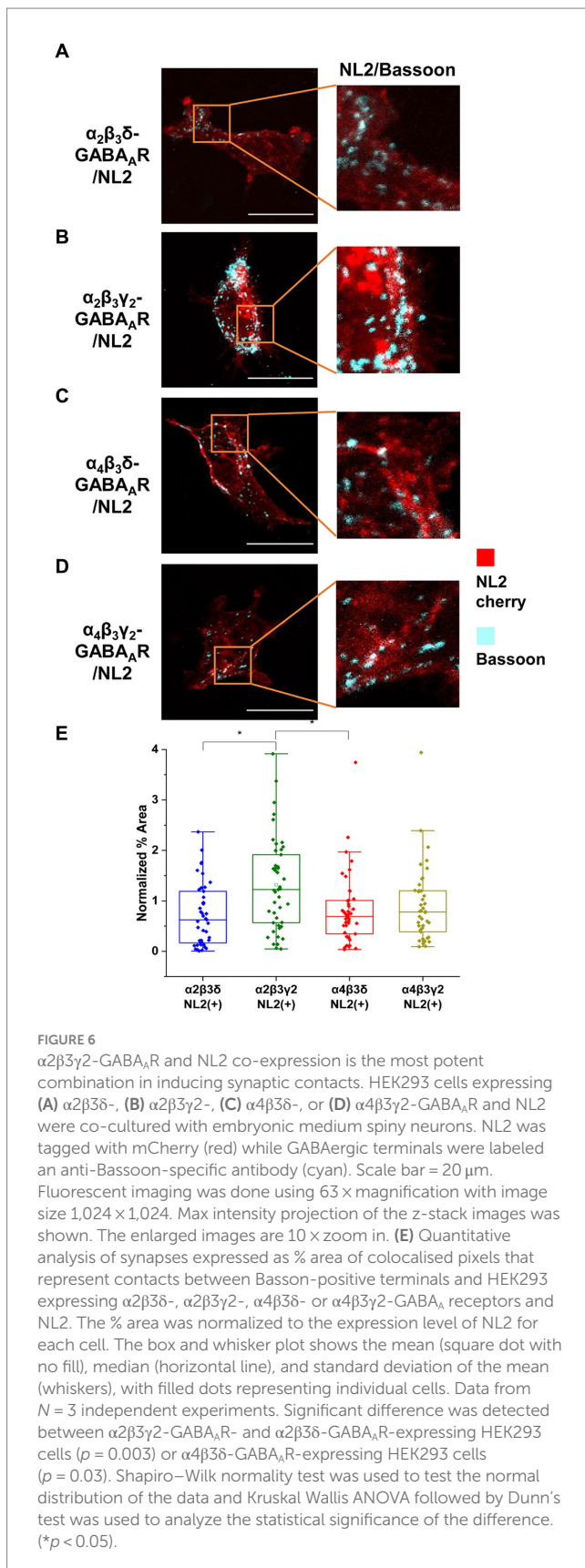
To investigate these differences further, we have also carried out immunolabeling experiments to characterize the degree of innervation of HEK293 cells expressing different subunit combinations (Figures 6A–D). Synaptic contacts were defined based on signal colocalization between the presynaptic Bassoon and postsynaptic NL2 (cyan and red channel in Figures 6A–D) and analyzed using ImageJ as described in the Methods. Quantification of the % area of co-localized pixels that represent contacts between the Bassoon-positive terminals and NL2 demonstrated that the level of presynaptic innervation was significantly higher in the presence of $\alpha 2\beta 3\gamma 2$ -GABA_ARs (median = 1.22%; IQR = 0.54 – 1.96%; $n = 45$) than $\alpha 2\beta 3\delta$ - (median = 0.62%; IQR = 0.17 – 1.19%; $n = 43$, $p = 0.003$) or $\alpha 4\beta 3\delta$ -GABA_ARs (median = 0.69%; IQR = 0.34 – 1.01%; $n = 43$, $p = 0.03$) (from $N = 3$ independent experiments; Figure 6E). The lower innervation for $\alpha 4\beta 3\gamma 2$ combination, detected by imaging, was surprising given its ability to mediate IPSCs in the presence of NL2 (Figures 5C,G,H), possibly reflecting the greater sensitivity of electrophysiology for detecting active synapses.

Together, our results point to a key role of the $\gamma 2$ subunit in facilitating the NL2-induced synapse formation and functional maturation in this co-culture model. Although adhesion of active

GABAergic terminals can be induced by NL2 in the presence of other GABA_AR subunit combinations, the highest degree of innervation and the tight functional coupling between the presynaptic release of GABA and the postsynaptic responses require the cooperation between the $\gamma 2$ subunit-containing GABA_ARs and NL2.

3.3 The synergism between GABA_ARs and NL2 does not require GABA_AR activity

To test if the GABA_AR activation by GABA may be required for the observed effects, the control, $\alpha 2\beta 2\gamma 2$ -GABA_AR or $\alpha 4\beta 3\delta$ -GABA_AR-expressing HEK293 cells were transiently transfected with GFP and cherry-NL2 cDNAs and plated together with the medium spiny neurons in the absence or presence of bicuculline, a GABA_AR competitive antagonist (Supplementary Figure S4). Quantification of the % area of co-localized VGAT and GFP pixels that represent contacts showed potentiation of NL2 effects by $\alpha 2\beta 2\gamma 2$ -GABA_ARs irrespective of whether the cultures were incubated with DMSO (control HEK293/NL2 cells: median = 1.68%; IQR = 0.54 – 2.57%; $n = 20$; $\alpha 2\beta 2\gamma 2$ -GABA_AR/NL2 cells: median = 4.21%; IQR = 2.00



– 7.11%; $n = 20$; from $N = 2$ independent experiments, $p = 0.01$) or bicuculline (control HEK293/NL2 cells: median = 1.11%; IQR = 0.43 – 2.00%; $n = 21$; $\alpha 2\beta 2\gamma 2$ -GABA_AR/NL2 cells: median = 2.28%;

IQR = 1.34 – 4.22%; $n = 20$, respectively; from $N = 2$ independent experiments, $p = 0.009$; [Supplementary Figures S4A,C](#)).

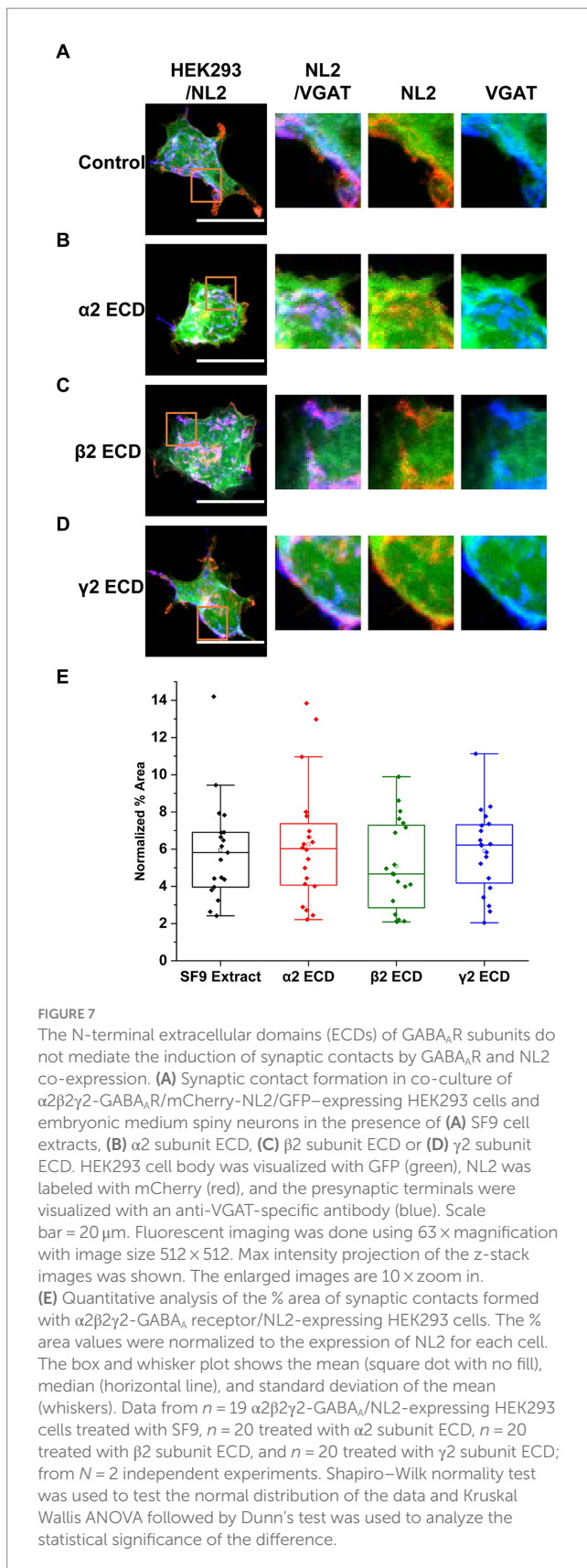
Similar results were obtained in co-cultures of control HEK293/NL2 and $\alpha 4\beta 3\delta$ -GABA_AR/NL2-expressing HEK293 cells in the absence or presence of bicuculline ([Supplementary Figures S4B,D](#)). Quantification of the % area of co-localized pixels of VGAT and GFP that represent contacts between the presynaptic terminals and HEK293 cells showed a significant increase in NL2 induction in the presence of $\alpha 4\beta 3\delta$ -GABA_AR in both DMSO-treated cultures (control HEK293/NL2 cells: median = 1.05% IQR = 0.52 – 1.72%; $n = 20$; $\alpha 4\beta 3\delta$ -GABA_AR/NL2 cells: median = 2.89% IQR = 1.77 – 4.99%; $n = 20$; from $N = 2$ independent experiments, $p = 0.03$) and bicuculline-treated cultures (control HEK293/NL2 cells: median = 1.05% IQR = 0.27 – 1.27%; $n = 20$; from $N = 2$ independent experiments; $\alpha 4\beta 3\delta$ -GABA_AR/NL2 cells: median = 3.23% IQR = 1.36 – 4.79%; $n = 20$; from $N = 2$ independent experiments, $p = 0.03$; [Supplementary Figure S4D](#)).

3.4 GABA_ARs and NL2 synergism is mediated by the TM3–4 intracellular loop of the $\gamma 2$ subunit

To investigate the mechanisms underlying the observed synergistic effects of $\alpha 2\beta 2\gamma 2$ -GABA_ARs and NL2 in synapse formation, we first assessed whether the extracellular N-terminal domains (ECDs) of GABA_AR $\alpha 2$, $\beta 2$ or $\gamma 2$ subunits may be involved given that they were previously shown to contribute to the GABAergic synapse formation in the absence of NL2 ([Figure 7](#); [Brown et al., 2016](#)).

To test this, 4 μ g of either the $\alpha 2$ ([Figure 7B](#)), $\beta 2$ ([Figure 7C](#)), or $\gamma 2$ ECD ([Figure 7D](#); 0.29–0.32 μ M), purified from SF9 cells ([Brown et al., 2016](#)) were applied to the co-culture of $\alpha 2\beta 2\gamma 2$ -GABA_AR/GFP/NL2-expressing HEK293 cells and medium spiny neurons. An equivalent amount of untransfected SF9 cell extract (4 μ g), following the same purification procedure as the extracts expressing ECDs, was used as a control ([Figure 7A](#)). Quantification of the % area of co-localized pixels of VGAT and GFP that represent synaptic contacts showed no significant change with the application of ECDs ([Figure 7E](#)). With SF9 extract control, the median was 5.82% (IQR = 3.96 – 6.90%, $n = 19$ cells from $N = 2$ independent experiments). Application of $\beta 2$ ECD slightly decreased the synapse formation albeit not significantly (median = 4.67%; IQR = 2.67 – 7.35%; $n = 20$ cells; from $N = 2$ independent experiments). No change was observed with the application of $\alpha 2$ (median = 6.03%; IQR = 4.04 – 7.58%; $n = 20$ cells; from $N = 2$ independent experiments) or $\gamma 2$ (median = 6.22%; IQR = 4.05 – 7.33%; $n = 20$ cells; from $N = 2$ independent experiments) ECDs.

These results indicate that cooperation between $\alpha 2\beta 2\gamma 2$ -GABA_ARs and NL2 may be mediated by the subunit intracellular domains. To test this hypothesis, we took advantage of previously characterized δ - $\gamma 2$ subunits chimera ([Hannan et al., 2020](#)), in which the large intracellular loop (ICL) (TM 3–4) of the δ subunit was replaced with the equivalent domain of the $\gamma 2$ subunit ($\delta\gamma 2$ ICL). HEK293 cells stably expressing $\beta 3$ subunits were transiently transfected with the cherry-NL2 and $\alpha 2 + \gamma 2$ ([Figure 8A](#)), or $\alpha 2 + \delta\gamma 2$ ICL ([Figure 8B](#)), or $\alpha 2 + \delta$ ([Figure 8C](#)) cDNAs and cultured with medium spiny neurons for 24h. Quantification of the % area of co-localized pixels that represent contacts between presynaptic Bassoon and NL2 demonstrated no significant difference in NL2-dependent induction



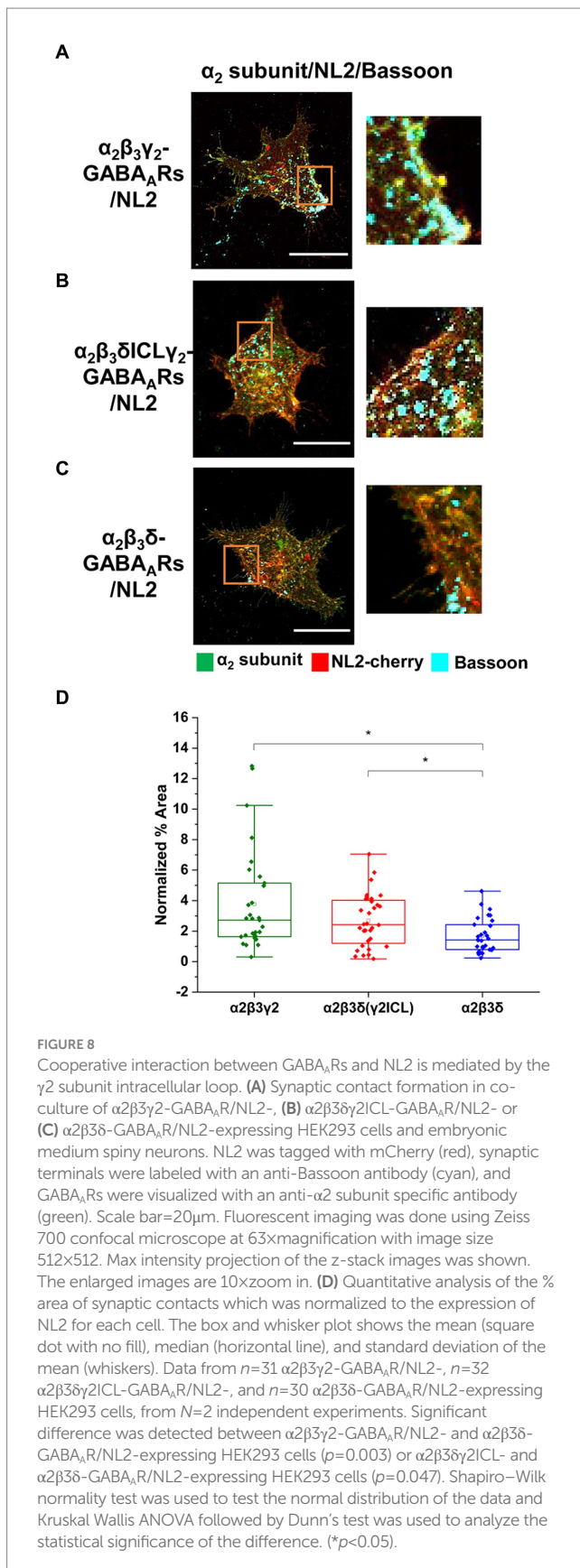
of synaptic contacts between the $\alpha 2\beta 3\gamma 2$ /NL2 and $\alpha 2\beta 3\delta\gamma 2$ ICL/NL2 (median = 2.72%; IQR = 1.63 – 5.15%; $n = 31$ cells, versus median = 2.42%; IQR = 1.12 – 4.06%; $n = 32$ cells; $N = 2$ independent

experiments). In both conditions, the NL2 effects were significantly greater than in the presence of $\alpha 2\beta 3\delta$ -GABA_ARs (median = 1.42%; IQR = 0.78 – 2.49%; $n = 30$ cells, respectively, $p = 0.003$ for $\alpha 2\beta 3\gamma 2$ /NL2, $p = 0.047$ for $\alpha 2\beta 3\delta\gamma 2$ ICL/NL2; $N = 2$ independent experiments; Figure 8D). Thus, the TM3-4 intracellular loop of the $\gamma 2$ subunit mediates the cooperativity between GABA_ARs and NL2. Whether the large intracellular loop of the $\gamma 2$ subunit mediated a direct interaction between the GABA_ARs and NL2 remained unclear.

To address this question, we have carried out co-immunoprecipitation experiments using the lysates of HEK293 cells expressing Myc-tagged $\alpha 2\beta 3\gamma 2$ -GABA_ARs and HA-tagged NL2. Using either the Myc-antibody, followed by immunoblotting with the NL2-specific antibody (Figure 9A), or, conversely, HA-tag antibody, followed by immunoblotting with $\beta 3$ subunit-specific antibody (Figure 9B), we confirmed that GABA_ARs and NL2 can be co-immunoprecipitated and thus can interact with each other. Furthermore, to assess if the ICL of $\gamma 2$ subunit mediates this interaction, $\alpha 2\beta 3\gamma 2$ -, or $\alpha 2\beta 3\delta\gamma 2$ ICL- or $\alpha 2\beta 3\delta$ -GABA_ARs were co-expressed with HA-tagged NL2 in HEK293 cells, and subjected to co-immunoprecipitation with the Myc-antibody followed by immunoblotting with the NL2-antibody or $\beta 3$ -subunit antibody. In $\alpha 2\beta 3\gamma 2$ -GABA_AR precipitates, a clear band corresponding to the molecular weight for NL2 was detected while no such band was detected in $\alpha 2\beta 3\delta$ -GABA_AR precipitates (Figure 9C, upper panel). In the $\alpha 2\beta 3\delta\gamma 2$ ICL-GABA_AR precipitates, a weaker band corresponding to NL2 was also detected (Figure 9C, upper panel). Immunoblotting with the $\beta 3$ subunit antibody showed that the amount of precipitated GABA_ARs was comparable in three different conditions (Figure 9C, lower panel). To test if NL2 can bind directly to the large intracellular domain of the $\gamma 2$ subunit, GST-tagged ICL was expressed and purified from *E. coli* and incubated with the lysates of HEK293 cells transfected with HA-NL2. However, the binding between NL2 and the TM 3–4 ICL of the $\gamma 2$ subunit (Figure 9D) could not be detected, indicating that GABA_ARs and NL2 interaction may be indirect and likely mediated by another protein, the nature of which remains to be established. Nevertheless, GABA_ARs and NL2 can interact *in vivo* as demonstrated by their co-immunoprecipitation from rat brain lysates prepared under non-denaturing conditions (Figure 9E).

4 Discussion

GABA_ARs and NL2 are co-expressed in many GABAergic inhibitory synapses in the mammalian brain with both proteins being implicated in synaptic initiation and functional maturation (Ali et al., 2020). It is now evident that together with many other proteins, GABA_ARs and NL2 undergo complex interactions to facilitate synaptic contact formation but how these interactions are coordinated in time and space to lead to the establishment of fully functional inhibitory synapses remains to be described in detail. This is important because genetic mutations and alterations in NL2 and GABA_ARs expression and function found in patients have been directly associated with their neurological and psychiatric symptoms, often showing a degree of overlap (Ali et al., 2020; Thompson, 2024). In many such cases, deficits in inhibitory synaptic connections have been implicated as the leading cause of the symptoms that patients experience. However, the intricate details of molecular interactions with a clear functional read-out are difficult to study in complex *in vivo* or *in vitro* systems in which these



and many other proteins coexist. The current study therefore aimed to investigate whether and how the interaction between GABA_ARs and NL2 may lead to the establishment of functional synapses in the

absence of other synaptic proteins using a reduced *in vitro* co-culture system. Although far from the situation *in vivo* and subject to the limitations of any study in a reduced system, this approach has revealed a synergism between GABA_ARs and NL2 in inducing synaptic formations for which the presence of the γ_2 subunit and specifically its TM3-4 intracellular domain-mediated interaction between these proteins are required.

We also know that the phosphorylation status of NL2 is important for its surface stability and for regulating synaptic GABA_AR numbers at synapses (Half et al., 2022). Furthermore, we and others have previously shown that the number of synaptic contacts could be enhanced significantly by co-expression of NL2 and GABA_ARs in heterologous co-culture models (Fuchs et al., 2013) and cultured neurons (Fu and Vicini, 2009). Moreover, in functional experiments, synaptic responses including spontaneous IPSC and miniature IPSC amplitudes detected in the presence of NL2 (and GABA_ARs) indicated that each nerve terminal elicits a more efficacious postsynaptic response and that each axon forms more functional synapses. Our current study largely confirms these findings but also draws an important distinction between the synaptic and extrasynaptic subtypes of GABA_ARs in their ability to synergize with NL2. The synaptic GABA_ARs, those more closely associated with NL2 *in vivo*, show a significantly stronger synergism with NL2 in synaptic initiation and pre- and post-synaptic coupling leading to the formation of fully functional synapses. The extrasynaptic δ -GABA_ARs, although able to potentiate the synaptogenic effects of NL2 to some extent, do not generate the same postsynaptic responses as their γ_2 counterparts, probably due to their largely perisynaptic localization rather than their intrinsic channel properties given that they have a higher affinity for GABA and slower desensitization rate than synaptic GABA_ARs (Farrant and Nusser, 2005; Mortensen et al., 2011). This infers that synaptic GABA_ARs may have a stronger physical association with NL2 than the extrasynaptic receptors which is indeed supported by our biochemical experiments showing that NL2 could be detected only in precipitated protein complexes of synaptic GABA_ARs.

Our current study also confirms the previously reported synaptogenic activity of synaptic GABA_ARs in the absence of NL2 (Fuchs et al., 2013; Brown et al., 2014, 2016). These *in vitro* findings are supported by the *in vivo* evidence from GABA_AR α_1 , α_3 or γ_2 subunit knock-out mice demonstrating that the lack of these subunits in certain brain regions leads to prominent structural changes in specific types of inhibitory synapses (Schweizer et al., 2003; Li et al., 2005; Fritschy and Panzanelli, 2006; Studer et al., 2006). Moreover, genetic deletion of GABA_ARs using CRISPR-Cas9 technology in a single hippocampal neuron was shown to cause a substantial reduction in GABAergic synapses received by this cell (Duan et al., 2019), further supporting the critical role of GABA_ARs in inhibitory synapse development.

NL2 has been viewed as a chief synaptic adhesion mediator based on its well-characterized interactions with the presynaptic proteins Neurexins (Sudhof, 2008), although many other adhesion proteins have also been shown to facilitate the initiation of synaptic contacts (Connor and Siddiqui, 2023). However, the presence of GABA_ARs is the key requirement for these contacts to develop into functional synapses. Moreover, in the presence of synaptic GABA_ARs and NL2 at the postsynaptic membrane, significantly more presynaptic GABAergic terminals show the activity-dependent uptake of synaptotagmin luminal domain-specific antibodies indicating that their ability to release GABA is enhanced in comparison with the

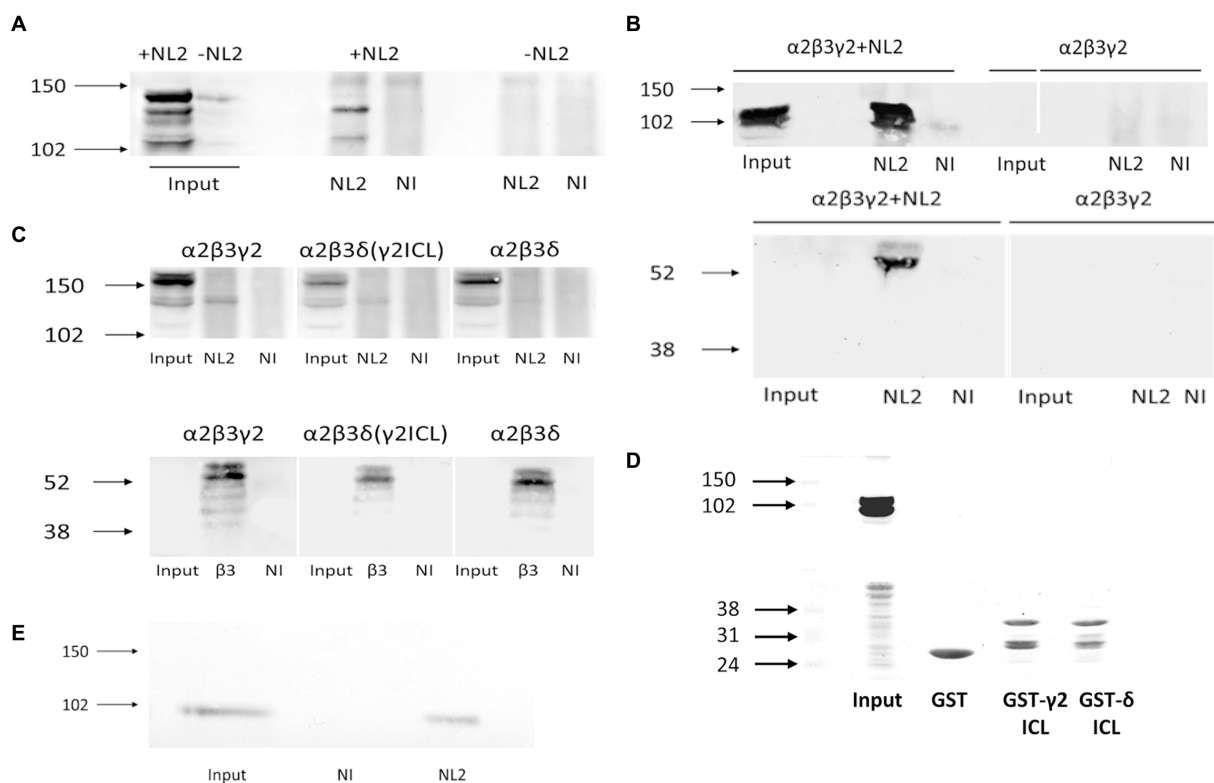


FIGURE 9

GABA_AR and NL2 interaction is mediated by the $\gamma 2$ subunit intracellular loop. (A) Myc-tagged GABA_ARs were immunoprecipitated using a myc-specific antibody, followed by detection of NL2 by immunoblotting using an anti-NL2-specific antibody. (B) HA-tagged NL2 was immunoprecipitated with a HA-specific antibody and subsequently detected by immunoblotting with the same antibody (upper panel), while the presence of GABA_ARs in precipitates was detected by immunoblotting with an anti- $\beta 3$ specific antibody (lower panel). (C) NL2-GABA_A receptor interaction in the presence of the $\gamma 2$ subunit intracellular TM 3–4 loop domain detected by co-immunoprecipitation. The $\beta 3$ subunit was myc-tagged. The immunoprecipitation was carried out with an anti-myc-specific antibody. NL2 was detected in precipitates using an anti-NL2-specific antibody (upper panel), while GABA_A receptors were detected using an anti- $\beta 3$ subunit-specific antibody (lower panel). (D) NL2 does not bind to the purified GST- $\gamma 2$ ICL or GST- δ ICL *in vitro* (upper panel). Purified GST fusion proteins were detected by Ponceau S (lower panel). (E) NL2 interacts with GABA_ARs in the adult male rat cortex. Co-immunoprecipitation was carried out with an anti- $\alpha 1$ subunit C-terminal-specific antibody, followed by detection of NL2 by immunoblotting using an anti-NL2-specific antibody. In all immunoblotting experiments, the binding of primary antibodies was visualized using alkaline phosphatase-conjugated secondary antibody and NBT/BCIP color substrate reaction. Blots are representative of $N = 2$ independent experiments for each experimental paradigm.

conditions where only NL2 or GABA_ARs are expressed. This suggests that GABA_ARs also influence presynaptic maturation regulated by NL2 either directly, by interacting with the presynaptic proteins such as Neurexins (Zhang et al., 2010) and/or other proteins involved in this process (Brown et al., 2016), or they act indirectly, by facilitating the NL2 interactions with its presynaptic partners. However, direct interactions of GABA_ARs with presynaptic proteins in this context are less likely to contribute because introducing the purified N-terminal ECDs of individual subunits as blocking reagents into our co-cultures did not affect the synergism between GABA_ARs and NL2. Nevertheless, it remains possible that GABA_ARs may still engage directly via interactions that require the fully assembled heteropentameric N-terminals ECDs rather than ECDs of individual subunits used in our experiments or they may act via their C-terminal ECDs. The indirect facilitation of presynaptic maturation by GABA_ARs is supported by our findings as well as by previous studies. Our results indicate that the intracellular TM3-4 loop of the $\gamma 2$ subunits is required for the cooperativity between GABA_ARs and NL2 in synaptic formation but also for the association between GABA_ARs and NL2.

However, the TM 3–4 ICL may not be sufficient for binding to occur, given that no binding to NL2 was detected when the purified GST-fusion of the $\gamma 2$ TM3-4 intracellular loop was tested in binding assays *in vitro*. It is therefore likely that this association is mediated by another protein that can bind directly to both the $\gamma 2$ TM3-4 intracellular loop and NL2. While there may be several proteins involved, one of the two main candidates is the tetraspanin LHFPL4, also known as GARLH4, which interacts with the $\gamma 2$ subunit to link GABA_ARs and NL2 (Davenport et al., 2017; Yamasaki et al., 2017; Han et al., 2021). However, the attempts to detect this protein in our HEK293 cell lines using immunoblotting with specific antibodies were unsuccessful (data not shown), which leads us to conclude that this protein is unlikely to play a role in the synergism between GABA_ARs and NL2 observed in this study. The other main candidate for this role is the postsynaptic scaffold protein gephyrin which was shown previously to directly interact with the TM3-4 intracellular loops of multiple GABA_ARs subunits, including the $\gamma 2$ subunit (Tretter et al., 2008; Maric et al., 2011; Mukherjee et al., 2011; Tretter et al., 2011; Kowalczyk et al., 2013; Maric et al., 2014), but also NL2 (Antonelli

et al., 2014; Nguyen et al., 2016). Gephyrin is expressed in our HEK293 cell lines in abundance (data not shown) which suggests that the observed interaction between NL2 and GABA_ARs may be at least in part mediated by this protein.

It is also likely that multiple interactions between gephyrin and α (1, 2, 3 or 5), β (2 or 3) and γ 2 subunits incorporated into the synaptic subtypes of GABA_ARs occur at the same time and cumulatively contribute to a strong and stable binding of the receptor to gephyrin and NL2, which may be required for the initiation of synapses. In contrast, the extrasynaptic GABA_AR subtypes may still engage in interactions with gephyrin and indirectly with NL2 via their β subunits given that α 4, α 6, or δ do not bind gephyrin, but this interaction is likely to be weaker and transient and therefore insufficient to stabilize the complex between GABA_ARs and NL2 to the extent required for the formation of new functional synapses. This could potentially explain the findings that the initiation of contacts is still increased in the presence of extrasynaptic GABA_AR and NL2, but these contacts do not develop into functional synapses. The perisynaptic localization of these receptors shown in our study and previously (Wei et al., 2003; Farrant and Nusser, 2005) is in agreement with this hypothesis. Moreover, the transient nature of these interactions and the ability of extrasynaptic GABA_ARs to migrate laterally into and out of synapses even when synapses are established and fully functional has been demonstrated in a study which also showed that the TM3-4 loop of γ 2 subunit plays a key role in regulating the degree of lateral migration of synaptic GABA_ARs (Hannan et al., 2020). Finally, the apparent correlation between the degree of synergism between GABA_ARs and NL2 and the establishment of functional synapses led us to assess whether GABA_AR channel activity may contribute to these developmental processes as described previously (Chattopadhyaya et al., 2007; Arama et al., 2015; Oh et al., 2016). In the presence of bicuculline, the synergism between synaptic or extrasynaptic GABA_AR and NL2 in synaptic contact formation was unaffected which further supports our hypothesis that GABA_ARs not only mediate synaptic transmission in the brain but also participate together with NL2 in the initiation and maturation of synaptic contacts as structural proteins.

Data availability statement

The raw data supporting the conclusions of this article will be made available by the authors, without undue reservation.

Ethics statement

The animal study was approved by Ethics Committee University College London. The study was conducted in accordance with the local legislation and institutional requirements.

References

Ali, H., Marth, L., and Krueger-Burg, D. (2020). Neuroligin-2 as a central organizer of inhibitory synapses in health and disease. *Sci. Signal.* 13:379. doi: 10.1126/scisignal.abd8379

Antonelli, R., Pizzarelli, R., Pedroni, A., Fritschy, J. M., Del Sal, G., Cherubini, E., et al. (2014). Pin1-dependent signalling negatively affects GABAergic transmission by

Author contributions

YS: Writing – review & editing, Methodology, Investigation, Formal analysis, Data curation, Conceptualization. MM: Writing – review & editing, Methodology, Investigation, Formal analysis, Data curation. BY: Writing – review & editing, Methodology, Investigation, Formal analysis. MN: Writing – review & editing, Methodology. TS: Funding acquisition, Writing – review & editing, Supervision, Conceptualization. JJ: Writing – review & editing, Writing – original draft, Supervision, Project administration, Methodology, Funding acquisition, Formal analysis, Conceptualization.

Funding

The author(s) declare that financial support was received for the research, authorship, and/or publication of this article. This work was supported by the Medical Research Council United Kingdom (G0800498; JJ) and Medical Research Council United Kingdom MR/T002581/1 (TS) and Wellcome Trust 217199/Z/19/Z (TS).

Acknowledgments

We would like to thank Professor Alex Thomson for her support and Professor Talvinder Sihra for proof reading the manuscript.

Conflict of interest

The authors declare that the research was conducted in the absence of any commercial or financial relationships that could be construed as a potential conflict of interest.

The author(s) declared that they were an editorial board member of *Frontiers*, at the time of submission. This had no impact on the peer review process and the final decision.

Publisher's note

All claims expressed in this article are solely those of the authors and do not necessarily represent those of their affiliated organizations, or those of the publisher, the editors and the reviewers. Any product that may be evaluated in this article, or claim that may be made by its manufacturer, is not guaranteed or endorsed by the publisher.

Supplementary material

The Supplementary material for this article can be found online at: <https://www.frontiersin.org/articles/10.3389/fncel.2024.1423471/full#supplementary-material>

modulating neuroligin2/gephyrin interaction. *Nat. Commun.* 5:5066. doi: 10.1038/ncomms6066

Arama, J., Abitbol, K., Goffin, D., Fuchs, C., Sihra, T. S., Thomson, A. M., et al. (2015). GABAA receptor activity shapes the formation of inhibitory synapses between

- developing medium spiny neurons. *Front. Cell. Neurosci.* 9:290. doi: 10.3389/fncel.2015.00290
- Brown, L. E., Fuchs, C., Nicholson, M. W., Stephenson, F. A., Thomson, A. M., and Jovanovic, J. N. (2014). Inhibitory synapse formation in a co-culture model incorporating GABAergic medium spiny neurons and HEK293 cells stably expressing GABAA receptors. *J. Vis. Exp.* 93:e52115. doi: 10.3791/52115
- Brown, L. E., Nicholson, M. W., Arama, J. E., Mercer, A., Thomson, A. M., and Jovanovic, J. N. (2016). Gamma-aminobutyric acid type A (GABAA) receptor subunits play a direct structural role in synaptic contact formation via their N-terminal extracellular domains. *J. Biol. Chem.* 291, 13926–13942. doi: 10.1074/jbc.M116.714790
- Chattopadhyaya, B., Di Cristo, G., Wu, C. Z., Knott, G., Kuhlman, S., Fu, Y., et al. (2007). GAD67-mediated GABA synthesis and signaling regulate inhibitory synaptic innervation in the visual cortex. *Neuron* 54, 889–903. doi: 10.1016/j.neuron.2007.05.015
- Cherubini, E., and Ben-Ari, Y. (2023). GABA signaling: therapeutic targets for neurodegenerative and neurodevelopmental disorders. *Brain Sci.* 13:1240. doi: 10.3390/brainsci13091240
- Chua, H. C., and Chebib, M. (2017). GABA(a) receptors and the diversity in their structure and pharmacology. *Adv. Pharmacol.* 79, 1–34. doi: 10.1016/bs.apha.2017.03.003
- Connolly, C. N., Krishek, B. J., McDonald, B. J., Smart, T. G., and Moss, S. J. (1996a). Assembly and cell surface expression of heteromeric and homomeric gamma-aminobutyric acid type A receptors. *J. Biol. Chem.* 271, 89–96. doi: 10.1074/jbc.271.1.89
- Connolly, C. N., Wooltorton, J. R., Smart, T. G., and Moss, S. J. (1996b). Subcellular localization of gamma-aminobutyric acid type A receptors is determined by receptor beta subunits. *Proc. Natl. Acad. Sci. U. S. A.* 93, 9899–9904. doi: 10.1073/pnas.93.18.9899
- Connor, S. A., and Siddiqui, T. J. (2023). Synapse organizers as molecular codes for synaptic plasticity. *Trends Neurosci.* 46, 971–985. doi: 10.1016/j.tins.2023.08.001
- Davenport, E. C., Pendolino, V., Kontou, G., Mcgee, T. P., Sheehan, D. F., Lopez-Domenech, G., et al. (2017). An essential role for the Tetraspanin LHFPL4 in the cell-type-specific targeting and clustering of synaptic GABA(a) receptors. *Cell Rep.* 21, 70–83. doi: 10.1016/j.celrep.2017.09.025
- Duan, J., Pandey, S., Li, T., Castellano, D., Gu, X., Li, J., et al. (2019). Genetic deletion of GABA(a) receptors reveals distinct requirements of neurotransmitter receptors for GABAergic and glutamatergic synapse development. *Front. Cell. Neurosci.* 13:217. doi: 10.3389/fncel.2019.00217
- Farrant, M., and Nusser, Z. (2005). Variations on an inhibitory theme: phasic and tonic activation of GABA(a) receptors. *Nat. Rev. Neurosci.* 6, 215–229. doi: 10.1038/nrn1625
- Fritschy, J. M., and Panzanelli, P. (2006). Molecular and synaptic organization of GABAA receptors in the cerebellum: effects of targeted subunit gene deletions. *Cerebellum* 5, 275–285. doi: 10.1080/14734220600962805
- Fritschy, J. M., and Panzanelli, P. (2014). GABAA receptors and plasticity of inhibitory neurotransmission in the central nervous system. *Eur. J. Neurosci.* 39, 1845–1865. doi: 10.1111/ejn.12534
- Fritschy, J. M., Panzanelli, P., and Tyagarajan, S. K. (2012). Molecular and functional heterogeneity of GABAergic synapses. *Cell. Mol. Life Sci.* 69, 2485–2499. doi: 10.1007/s00018-012-0926-4
- Fu, Z., and Vicini, S. (2009). Neuroligin-2 accelerates GABAergic synapse maturation in cerebellar granule cells. *Mol. Cell. Neurosci.* 42, 45–55. doi: 10.1016/j.mcn.2009.05.004
- Fuchs, C., Abitbol, K., Burden, J. J., Mercer, A., Brown, L., Iball, J., et al. (2013). GABA(a) receptors can initiate the formation of functional inhibitory GABAergic synapses. *Eur. J. Neurosci.* 38, 3146–3158. doi: 10.1111/ejn.12331
- Half, E. F., Hannan, S., Kwanthongdee, J., Lesept, F., Smart, T. G., and Kittler, J. T. (2022). Phosphorylation of neuroligin-2 by PKA regulates its cell surface abundance and synaptic stabilization. *Sci. Signal.* 15:eabg2505. doi: 10.1126/scisignal.abg2505
- Han, W., Shepard, R. D., and Lu, W. (2021). Regulation of GABA(a)Rs by transmembrane accessory proteins. *Trends Neurosci.* 44, 152–165. doi: 10.1016/j.tins.2020.10.011
- Hannan, S., Minere, M., Harris, J., Izquierdo, P., Thomas, P., Tench, B., et al. (2020). GABA(a)R isoform and subunit structural motifs determine synaptic and extrasynaptic receptor localisation. *Neuropharmacology* 169:107540. doi: 10.1016/j.neuropharm.2019.02.022
- Klausberger, T., Roberts, J. D., and Somogyi, P. (2002). Cell type- and input-specific differences in the number and subtypes of synaptic GABA(a) receptors in the hippocampus. *J. Neurosci.* 22, 2513–2521. doi: 10.1523/JNEUROSCI.22-07-02513.2002
- Kowalczyk, S., Winkelmann, A., Smolinsky, B., Forstera, B., Neundorff, I., Schwarz, G., et al. (2013). Direct binding of GABAA receptor beta2 and beta3 subunits to gephyrin. *Eur. J. Neurosci.* 37, 544–554. doi: 10.1111/ejn.12078
- Li, J., Han, W., Pelkey, K. A., Duan, J., Mao, X., Wang, Y. X., et al. (2017). Molecular dissection of Neuroligin 2 and Slitrk3 reveals an essential framework for GABAergic synapse development. *Neuron* 96:e8. doi: 10.1016/j.neuron.2017.10.003
- Li, R. W., Yu, W., Christie, S., Miralles, C. P., Bai, J., Loturco, J. J., et al. (2005). Disruption of postsynaptic GABA receptor clusters leads to decreased GABAergic innervation of pyramidal neurons. *J. Neurochem.* 95, 756–770. doi: 10.1111/j.1471-4159.2005.03426.x
- Lorenz-Guertin, J. M., Bambino, M. J., and Jacob, T. C. (2018). gamma2 GABA(a)R trafficking and the consequences of human genetic variation. *Front. Cell. Neurosci.* 12:265. doi: 10.3389/fncel.2018.00265
- Maric, H. M., Kasaragod, V. B., Hausrat, T. J., Kneussel, M., Tretter, V., Stromgaard, K., et al. (2014). Molecular basis of the alternative recruitment of GABA(a) versus glycine receptors through gephyrin. *Nat. Commun.* 5:5767. doi: 10.1038/ncomms6767
- Maric, H. M., Mukherjee, J., Tretter, V., Moss, S. J., and Schindelin, H. (2011). Gephyrin-mediated gamma-aminobutyric acid type A and glycine receptor clustering relies on a common binding site. *J. Biol. Chem.* 286, 42105–42114. doi: 10.1074/jbc.M111.303412
- Mortensen, M., Patel, B., and Smart, T. G. (2011). GABA potency at GABA(a) receptors found in synaptic and Extrasynaptic zones. *Front. Cell. Neurosci.* 6:1. doi: 10.3389/fncel.2012.00001
- Mortensen, M., and Smart, T. G. (2007). Single-channel recording of ligand-gated ion channels. *Nat. Protoc.* 2, 2826–2841. doi: 10.1038/nprot.2007.403
- Mukherjee, J., Kretschmannova, K., Gouzer, G., Maric, H. M., Ramsden, S., Tretter, V., et al. (2011). The residence time of GABA(a)Rs at inhibitory synapses is determined by direct binding of the receptor alpha1 subunit to gephyrin. *J. Neurosci.* 31, 14677–14687. doi: 10.1523/JNEUROSCI.2001-11.2011
- Nguyen, Q. A., Horn, M. E., and Nicoll, R. A. (2016). Distinct roles for extracellular and intracellular domains in neuroligin function at inhibitory synapses. *eLife* 5:236. doi: 10.7554/eLife.19236
- Nguyen, Q. A., and Nicoll, R. A. (2018). The GABA(a) receptor beta subunit is required for inhibitory transmission. *Neuron* 98:e3. doi: 10.1016/j.neuron.2018.03.046
- Oh, W. C., Lutz, S., Castillo, P. E., and Kwon, H. B. (2016). De novo synaptogenesis induced by GABA in the developing mouse cortex. *Science* 353, 1037–1040. doi: 10.1126/science.aaf5206
- Olsen, R. W., and Sieghart, W. (2009). GABA A receptors: subtypes provide diversity of function and pharmacology. *Neuropharmacology* 56, 141–148. doi: 10.1016/j.neuropharm.2008.07.045
- Owens, D. F., and Kriegstein, A. R. (2002). Is there more to GABA than synaptic inhibition? *Nat. Rev. Neurosci.* 3, 715–727. doi: 10.1038/nrn919
- Pallotto, M., and Deprez, F. (2014). Regulation of adult neurogenesis by GABAergic transmission: signaling beyond GABAA-receptors. *Front. Cell. Neurosci.* 8:166. doi: 10.3389/fncel.2014.00166
- Raimondo, J. V., Richards, B. A., and Woodin, M. A. (2017). Neuronal chloride and excitability - the big impact of small changes. *Curr. Opin. Neurobiol.* 43, 35–42. doi: 10.1016/j.conb.2016.11.012
- Rudolph, U., and Mohler, H. (2006). GABA-based therapeutic approaches: GABAA receptor subtype functions. *Curr. Opin. Pharmacol.* 6, 18–23. doi: 10.1016/j.coph.2005.10.003
- Sallard, E., Letourneur, D., and Legendre, P. (2021). Electrophysiology of ionotropic GABA receptors. *Cell. Mol. Life Sci.* 78, 5341–5370. doi: 10.1007/s00018-021-03846-2
- Scheiffele, P., Fan, J., Choi, J., Fetter, R., and Serafini, T. (2000). Neuroligin expressed in nonneuronal cells triggers presynaptic development in contacting axons. *Cell* 101, 657–669. doi: 10.1016/S0092-8674(00)80877-6
- Schofield, P. R., Darlison, M. G., Fujita, N., Burt, D. R., Stephenson, F. A., Rodriguez, H., et al. (1987). Sequence and functional expression of the GABA A receptor shows a ligand-gated receptor super-family. *Nature* 328, 221–227. doi: 10.1038/328221a0
- Schweizer, C., Balsiger, S., Bluethmann, H., Mansuy, I. M., Fritschy, J. M., Mohler, H., et al. (2003). The gamma 2 subunit of GABA(a) receptors is required for maintenance of receptors at mature synapses. *Mol. Cell. Neurosci.* 24, 442–450. doi: 10.1016/S1044-7431(03)00202-1
- Scott, S., and Aricescu, A. R. (2019). A structural perspective on GABA(a) receptor pharmacology. *Curr. Opin. Struct. Biol.* 54, 189–197. doi: 10.1016/j.sbi.2019.03.023
- Smart, T. G., and Mortensen, M. (2023). GABA_A receptors in textbook of ion channels volume II: Properties, function, and pharmacology of the Superfamilies. Boca Raton, FL: CRC Press.
- Smart, T. G., and Stephenson, F. A. (2019). A half century of gamma-aminobutyric acid. *Brain Neurosci. Adv.* 3:58249. doi: 10.1177/2398212819858249
- Studer, R., Von Boehmer, L., Haeggi, T., Schweizer, C., Benke, D., Rudolph, U., et al. (2006). Alteration of GABAergic synapses and gephyrin clusters in the thalamic reticular nucleus of GABAA receptor alpha3 subunit-null mice. *Eur. J. Neurosci.* 24, 1307–1315. doi: 10.1111/j.1460-9568.2006.05006.x
- Sudhof, T. C. (2008). Neuroligins and neuexins link synaptic function to cognitive disease. *Nature* 455, 903–911. doi: 10.1038/nature07456
- Sudhof, T. C. (2017). Synaptic Neuexin complexes: a molecular code for the logic of neural circuits. *Cell* 171, 745–769. doi: 10.1016/j.cell.2017.10.024
- Sudhof, T. C. (2018). Towards an understanding of synapse formation. *Neuron* 100, 276–293. doi: 10.1016/j.neuron.2018.09.040
- Thomas, P., Mortensen, M., Hosie, A. M., and Smart, T. G. (2005). Dynamic mobility of functional GABAA receptors at inhibitory synapses. *Nat. Neurosci.* 8, 889–897. doi: 10.1038/nn1483
- Thompson, S. M. (2024). Modulators of GABA(a) receptor-mediated inhibition in the treatment of neuropsychiatric disorders: past, present, and future. *Neuropsychopharmacology* 49, 83–95. doi: 10.1038/s41386-023-01728-8

- Thomson, A. M., and Jovanovic, J. N. (2010). Mechanisms underlying synapse-specific clustering of GABA(a) receptors. *Eur. J. Neurosci.* 31, 2193–2203. doi: 10.1111/j.1460-9568.2010.07252.x
- Tretter, V., Ehya, N., Fuchs, K., and Sieghart, W. (1997). Stoichiometry and assembly of a recombinant GABAA receptor subtype. *J. Neurosci.* 17, 2728–2737. doi: 10.1523/JNEUROSCI.17-08-02728.1997
- Tretter, V., Jacob, T. C., Mukherjee, J., Fritschy, J. M., Pangalos, M. N., and Moss, S. J. (2008). The clustering of GABA(a) receptor subtypes at inhibitory synapses is facilitated via the direct binding of receptor alpha 2 subunits to gephyrin. *J. Neurosci.* 28, 1356–1365. doi: 10.1523/JNEUROSCI.5050-07.2008
- Tretter, V., Kerschner, B., Milenkovic, I., Ramsden, S. L., Ramerstorfer, J., Saiepour, L., et al. (2011). Molecular basis of the gamma-aminobutyric acid a receptor alpha3 subunit interaction with the clustering protein gephyrin. *J. Biol. Chem.* 286, 37702–37711. doi: 10.1074/jbc.M111.291336
- Wei, W., Zhang, N., Peng, Z., Houser, C. R., and Mody, I. (2003). Perisynaptic localization of delta subunit-containing GABA(a) receptors and their activation by GABA spillover in the mouse dentate gyrus. *J. Neurosci.* 23, 10650–10661. doi: 10.1523/JNEUROSCI.23-33-10650.2003
- Yamasaki, T., Hoyos-Ramirez, E., Martenson, J. S., Morimoto-Tomita, M., and Tomita, S. (2017). GARLH family proteins stabilize GABA(a) receptors at synapses. *Neuron* 93:e6. doi: 10.1016/j.neuron.2017.02.023
- Zhang, C., Atasoy, D., Arac, D., Yang, X., Fucillo, M. V., Robison, A. J., et al. (2010). Neurexins physically and functionally interact with GABA(a) receptors. *Neuron* 66, 403–416. doi: 10.1016/j.neuron.2010.04.008